Inorganic Chemistry

Article

pubs.acs.org/IC

Synthesis of Silver(I) and Gold(I) Complexes Containing Enantiopure Pybox Ligands. First Assays on the Silver(I)-Catalyzed Asymmetric Addition of Alkynes to Imines

Gustavo M. Borrajo-Calleja,[†] Eire de Julián,[†] Esther Bayón,[†] Josefina Díez,[†] Elena Lastra,[†] Isabel Merino,[‡] and M. Pilar Gamasa*,[†]

[†]Departamento de Química Orgánica e Inorgánica, IUQOEM (Unidad Asociada al CSIC), Centro de Innovación en Química Avanzada (ORFEO−CINQA), Universidad de Oviedo, E-33006 Oviedo, Principado de Asturias, Spain

[‡]Unidad de Resonancia Magnética Nuclear, Servicios Científico-Técnicos de la Universidad de Oviedo, E-33006 Oviedo, Principado de Asturias, Spain

Supporting Information

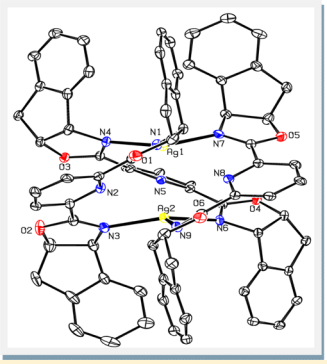

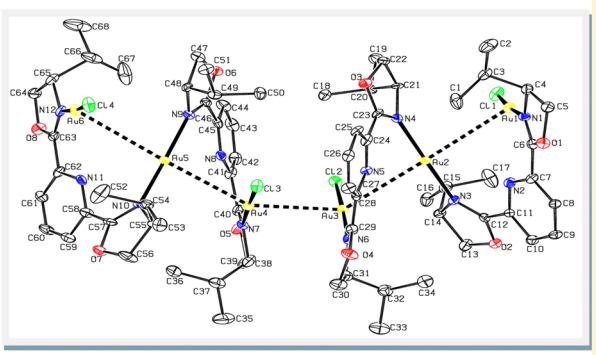

ABSTRACT: Dinuclear complexes $[Ag_2(CF_3SO_3)\{(S,S)\text{-}^i\text{Pr-pybox}\}_2][CF_3SO_3]$ (**1**), $[Ag_2(\text{R-pybox})_2][X]_2$ [R-pybox = 2,6-bis[4-(*S*)-isopropyloxazolin-2-yl]pyridine (*S*,*S*)-^{i}Pr-pybox and X = PF_6 (**2**) and BF_4 (**3**); R-pybox = 2,6-bis[(3a*S*,8a*R*)-8,8a-dihydro-3a*H*-indeno[1,2-*d*]oxazol-2-yl]pyridine (3a*S*,3a′*S*,8a*R*,8a′*R*)-indane-pybox and X = CF_3SO_3 (**4**)], $[Ag_2\{(S,S)\text{-}^i\text{Pr-pybox}\}\{(3aS,3a'S,8aR,8a'R)\text{-indane-pybox}\}][CF_3SO_3]_2$ (**5**), and $[Ag_2(\text{R-pybox})_3][X]_2$ [R-pybox = (3a*S*,3a′*S*,8a*R*,8a′*R*)-indane-pybox and X = CF_3SO_3 (**10**), SF_6 (**11**), and PF_6 (**12**)] as well as mononuclear complexes $[Ag(\text{R-pybox})_2][X]$ [R-pybox = (*S*,*S*)-^{i}Pr-pybox and X = SbF_6 (**6**), PF_6 (**7**), and BF_4 (**8**); R-pybox = (3a*S*,3a′*S*,8a*R*,8a′*R*)-indane-pybox) and X = BF_4 (**9**)] have been prepared by the reaction of the corresponding silver salts and pybox ligands using the appropriate molar ratio conditions. The first gold(I)/pybox complex $[Au_6Cl_4\{(S,S)\text{-}^i\text{Pr-pybox}\}_4][AuCl_2]_2$ (**13**) has been synthesized by the reaction of $[AuCl\{S(CH_3)_2\}]$ and (*S*,*S*)-^{i}Pr-pybox (1:1 molar ratio) in acetonitrile. The structures of the dinuclear (**1**, **4**, **5**, **10**, and **11**) and mononuclear (**6** and **9**) silver complexes and the hexanuclear gold complex **13** have been determined by single-crystal X-ray diffraction analysis. These studies have been complemented with a solution-state study by NMR spectroscopy, which included structure elucidation, variable-temperature measurements, and diffusion studies using diffusion-ordered spectroscopy (DOSY; for complexes **1**, **4**, **10**, and **12**). Complexes **1**, **2**, **4**, and **10** have been assayed as catalysts in the asymmetric addition of phenylacetylene to *N*-benzylideneaniline.

INTRODUCTION

The last years have witnessed a major advance in the use of enantiopure pybox-containing transition metals in the fundamental scenario of asymmetric synthesis.[1] In particular, pybox-containing copper(I) complexes have proven to be highly effective for asymmetric reactions. Thus, isolated[2,3] or in situ generated[4−12] copper(I) complexes have been shown to catalyze several asymmetric reactions, e.g., cyclopropanation of alkenes,[5] cycloaddition of azides with alkynes,[6] allylic oxidation of alkenes,[7] propargylic etherification of propargylic esters,[3] intramolecular propargylic amination of propargylic acetates,[8] propargylation of benzofuranones,[9] alkynylation of C,N-cyclic azomethine imines,[10] and addition of terminal alkynes to both α-iminophosphonates[11] and imines.[2,12] In addition, copper(II)/pybox complexes are able to catalyze the three-component coupling of aldehydes, amines, and alkynes[13] as well as the enantioselective Friedel−Crafts reaction of indoles.[14] On the contrary, examples of catalytic reactions involving other group 11 metal complexes containing enantiopure pybox ligands are very rare, and negligible enantiomeric excess (e.e.) has been reported.[15] A reason that might account for this gap deals with

Received: June 4, 2016

DOI: 10.1021/acs.inorgchem.6b01323
Inorg. Chem. XXXX, XXX, XXX−XXX

Scheme 1. Synthesis of the Dinuclear Complexes 1−4

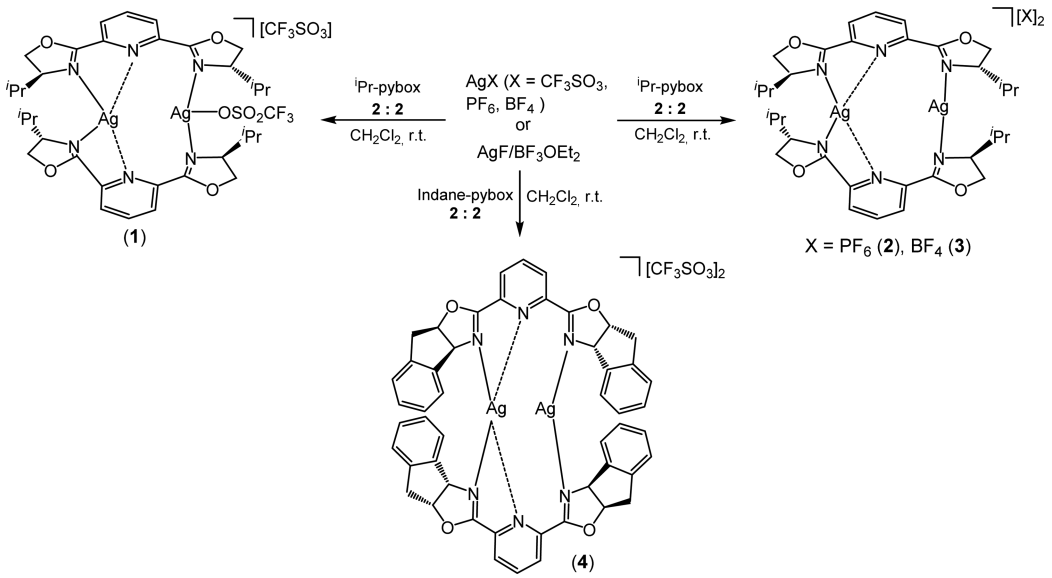

the lack of synthetic methods of these complexes. In this sense, it is relevant that, unlike the particular case of copper(I),[2,3,16] studies on the coordination chemistry of pybox with silver and gold metals are almost unknown because only the structures of the dinuclear and trinuclear silver(I) complexes $[Ag_2\{(S,S)\text{-Bz-pybox}\}_2][BF_4]_2$ and $[Ag_3\{(R,R)\text{-Ph-pybox}\}_3][BF_4]_3$ have been reported.[17,18]

In this paper, a simple and direct preparation of various enantiopure complexes of silver(I)- and gold(I)-containing pybox ligands is presented. Different mono- and dinuclear complexes of silver(I) have been selectively synthesized by using appropriate molar ratios of reactants. Furthermore, the first gold(I)/pybox complex that crystallizes as a hexanuclear species is described. Preliminary attempts toward the use of silver(I)/pybox complexes in asymmetric catalysis are performed, although only moderate results are reached.

RESULTS AND DISCUSSION

Synthesis of the Dinuclear Complexes $[Ag_2(CF_3SO_3)\{(S,S)\text{-}^iPr\text{-pybox}\}_2][CF_3SO_3]$ (1), $[Ag_2\{(S,S)\text{-}^iPr\text{-pybox}\}_2][X]_2$ [X = PF_6 (2) and BF_4 (3)], and $[Ag_2\{(3aS,3a'S,8aR,8a'R)\text{-indane-pybox}\}_2][CF_3SO_3]_2$ (4). The reaction of equimolar amounts of the corresponding silver salt AgX (X = CF_3SO_3, PF_6, and BF_4) with (*S*,*S*)-^{i}Pr-pybox and (3a*S*,3a′*S*,8a*R*,8a′*R*)-indane-pybox in dichloromethane at room temperature led to the dinuclear complexes **1**, **2**, and **4** in 50−84% yield. Complex **3** was alternatively synthesized by stirring a mixture of AgF, $BF_3{\cdot}OEt_2$, and ^{i}Pr-pybox (2:2:2 molar ratio) in dichloromethane at room temperature (66% yield; Scheme 1). All of the complexes reported in this paper were characterized by elemental analysis, molar conductivity, fast-atom-bombardment (FAB) mass spectrometry (MS; **1**, **4**, **6**, **9**, and **13**), and NMR spectroscopy (see the Experimental Section and Supporting Information for details). The molar conductivity value for complex **1** in nitromethane (86 S cm^2 mol^{-1}) or acetone (210 S cm^2 mol^{-1}) was in the expected range for 1:1 or 1:2 electrolytes in these solvents, respectively.[19] The Λ_M nitromethane value can be explained by assuming that the interaction of one triflate anion with a silver cation is maintained in a nitromethane solution. In fact, the interaction between one triflate anion and a silver cation was confirmed in solution and the solid state (see NMR studies and the crystal structure of complex **1**). The ^{1}H and ^{13}C NMR resonance signals of complexes **1**−**4** in solution (293 K) were fully consistent with the presence of a C_2-symmetry axis. Thus, the $^{13}C\{^1H\}$ NMR spectra for complexes **1**−**3** show single resonance signals for the OCH_2, OCN, and CH^iPr carbon atoms of both oxazoline rings and for the C3/C5 and C2/C6 carbon atoms of the pyridine ring. Similarly, single resonances for the OCN, OCH, and NCH carbon atoms of both oxazoline rings and for the C3/C5 and C2/C6 carbon atoms of the pyridine ring are observed in the case of complex **4** [see the variable-temperature (VT)-NMR experiments and diffusion studies undertaken for **1** and **4**]. Attempts at the synthesis of the analogous dicationic complex starting from $AgSbF_6$ were unsuccessful because an unidentified solid was formed whose ^{1}H NMR spectrum showed very broad peaks. All attempts to crystallize this solid from mixtures of different solvents resulted in the formation of the mononuclear complex **6** (see below).

The structures of complexes **1** and **4** were confirmed by single-crystal X-ray analyses. Complexes **1** and **4** crystallize in chiral space group $P2_12_12_1$ with Flack parameters of −0.011(5) and −0.020(4), respectively. In the same manner, all of the complexes described in this paper crystallize in chiral space groups because of the presence of an enantiopure ligand. In all cases, the Flack parameter was found to be nearly zero after refinement[20] (see Tables 2−4). The asymmetric unit of complex **1** consists of two molecules that have similar relevant structural parameters, and therefore only the data corresponding to one of them are discussed. ORTEP-type views of the cation of one of the molecules of **1** and the cation of **4** are shown in Figures 1 and 2, respectively. Selected bonding data are listed in Table 1. The structure of complex **1** shows a dimeric cation $[Ag_2(CF_3SO_3)\{(S,S)\text{-}^iPr\text{-pybox}\}_2]^+$ and one uncoordinated $CF_3SO_3^-$ anion, whereas the structure of complex **4** shows a dimeric dication $[Ag_2\{(3aS,3a'S,8aR,8a'R)\text{-indane-pybox}\}_2]^{2+}$ and two uncoordinated $CF_3SO_3^-$ anions. The lack of interaction between the silver atoms and triflate anions in the case of complex **4** might be attributed to the higher steric demand of the (3a*S*,3a′*S*,8a*R*,8a′*R*)-indane-pybox ligand versus the (*S*,*S*)-^{i}Pr-pybox

DOI: 10.1021/acs.inorgchem.6b01323
Inorg. Chem. XXXX, XXX, XXX−XXX

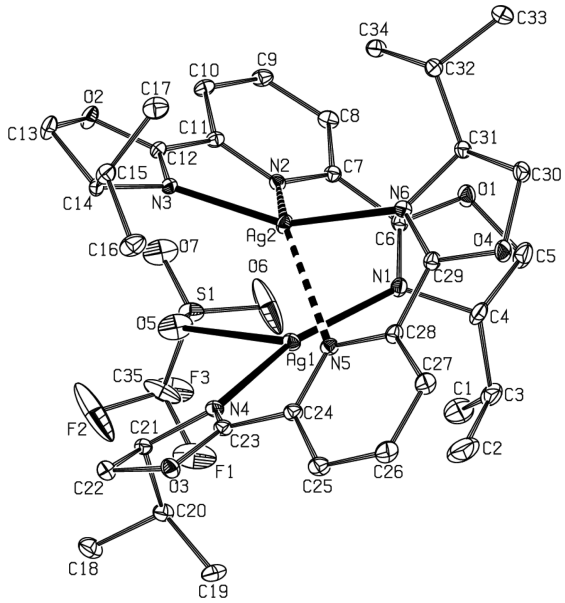

Figure 1. ORTEP drawing of the cationic complex **1** showing the atom-labeling scheme. Thermal ellipsoids are shown at the 10% probability level. Hydrogen atoms and the CF_3SO_3 anion are omitted for clarity.

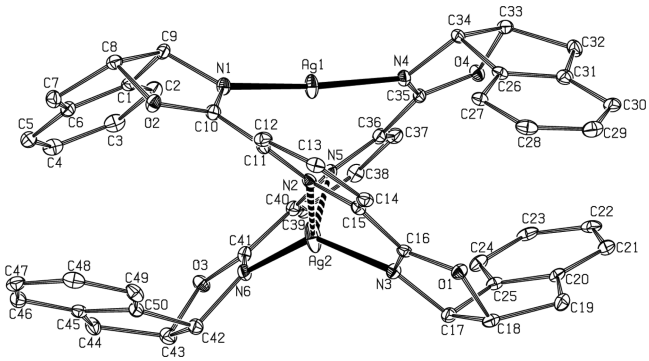

Figure 2. ORTEP drawing of the cationic complex **4** showing the atom-labeling scheme. Thermal ellipsoids are shown at the 20% probability level. Hydrogen atoms and the CF_3SO_3 anions are omitted for clarity.

ligand. In the case of complex **1**, the Ag1 and Ag2 atoms are coordinated to two oxazoline nitrogen atoms of two different pybox ligands with angle values of 157.4(2)° for N1−Ag1−N4 and 155.1(2)° for N3−Ag2−N6. These angles are quite different from the idealized linear value of 180° due to the coordination of a triflate group and pyridine nitrogen atoms (N2 and N5) to the Ag1 and Ag2 metal centers, respectively.[21] The four Ag−$N_{oxazoline}$ bond lengths are in the range of 2.183(6)−2.203(6) Å (av. 2.1915 Å) and are similar to those observed in other silver(I) oxazoline complexes (usually found in the range of 1.97−2.18 Å).[21,22] The Ag1−O5 bond distance [2.562(10) Å] is longer than the sum of the covalent radii for silver and oxygen atoms (2.11 Å)[23] but in the range found for other silver(I) triflate complexes (Ag−O, with a range of 2.67−2.362 Å).[24] The Ag2−$N_{pyridine}$ bond lengths [Ag2−N5 2.510(6) Å; Ag2−N2 2.6476(6) Å] are longer than those reported for other silver(I) pyridine complexes [av. 2.24 Å, range of 2.138(3)−2.391(1) Å].[25]

On the other hand, the Ag1 and Ag2 atoms in complex **4** are also coordinated to two oxazoline nitrogen atoms of two different indane-pybox ligands with angle values of 172.78(19)° for N1−Ag1−N4 and 140.54(18)° for N3−Ag1−N6. The coordination of the Ag1 atom is near linearity while that of the Ag2 atom is not strictly linear because of weak interactions with pyridine nitrogen groups [Ag2−N5 2.794(3) Å; Ag2−N2 2.683(3) Å]. These distances are larger than those found in complex **1** (Ag2−$N_{pyridine}$ av. 2.579 Å) but shorter than the sum of the van der Waals radii of silver and nitrogen atoms (3.27 Å).[26] The distances Ag−$N_{oxazoline}$ are sligthly shorter for the dicoordinate Ag1 atom [Ag1−N1 2.090(4) Å; Ag1−N4 2.087(4) Å] than for the Ag2 atom [Ag2−N3 2.152(4) Å; Ag2−N6 2.146(4) Å], whereas the silver(1) triflate coordination in complex **1** makes the four distances Ag−$N_{oxazoline}$ be very close to each other (see above). All of the $N_{oxazoline}$−Ag^{I} distances in complexes **1** and **4** are typical of covalent bonds.[23] Moreover, complexes **1** and **4** show also very weak interactions between the pyridine nitrogen atoms and the Ag1 atom [av. 2.985 Å (**1**), 3.055 Å (**4**)], although these distances are shorter than the sum of the van der Waals radii of silver and nitrogen atoms (3.27 Å).[26]

The Ag1···Ag2 distance is slightly shorter for complex **1** [2.8885(9) Å] than for complexes **4** [3.0295(9) Å] and $[Ag_2\{(S,S)\text{-Bz-pybox}\}_2][BF_4]_2$ [2.985(1) Å].[17] These distances are in the range expected for the sum of the covalent radii of two Ag atoms and suggest a significant argentophilic interaction between the silver atoms.[27] The Ag−Ag distances observed in complexes exhibiting argentophilic interactions are commonly found in the range of the sum of the covalent radii of two Ag atoms (2.90 Å)[23] and the 2-fold van der Waals radius of silver (3.44 Å).[26]

Remarkably, the pybox skeleton is not planar in complexes **1** and **4**, with the two pybox ligands being twisted around the Ag1−Ag2 axis, thus generating a double-helical structure with *P* (**1**) and *M* (**4**) helicity.[28] The torsion angle N−C−C−N values of the pybox ligands for complexes **1** and **4** are in the ranges of 8.3(13)−35.7(12)° (**1**) and −35.0(8) to −11.7(8)° (**4**). The cation units of complexes **1** and **4** were formed as single diastereoisomers *P*(*S*,*S*)(*S*,*S*) (**1**) and *M*(3a*S*,3a′*S*,8a*R*,8a′*R*)-(3a*S*,3a′*S*,8a*R*,8a′*R*) (**4**).

Synthesis of the Dinuclear Complex $[Ag_2\{(S,S)\text{-}^{i}Pr\text{-pybox}\}\{(3aS,3a'S,8aR,8a'R)\text{-indane-pybox}\}][CF_3SO_3]_2$ (5). When a mixture of $AgOSO_2CF_3$, (*S*,*S*)-^{i}Pr-pybox, and (3a*S*,3a′*S*,8a*R*,8a′*R*)-indane-pybox (2:1:1 molar ratio) was stirred in dichloromethane at room temperature, the dinuclear mixed complex **5** was isolated in moderate yield (56%) as the sole reaction product (Scheme 2). No traces of complexes **1** or **4** were detected.

The room temperature ^{1}H NMR spectrum of complex **5** shows the $CHMe_2$ group of ^{i}Pr-pybox appearing at much higher field [0.50 (CH*Me*$_2$), 0.48 (CH*Me*$_2$), −0.01 (m, C*H*Me$_2$) ppm] than that in the case of complex **1** [1.48 (C*H*Me$_2$), 0.91 (CH*Me*$_2$), 0.83 (CH*Me*$_2$) ppm] probably because of the shielding ring current effect of the indane group.[29] The structure of complex **5** was determined by single-crystal X-ray analysis, and selected bonding data are shown in Table 1. The asymmetric unit of complex **5** consists of two molecules that have similar relevant structural parameters. The ORTEP-type view of the dication $[Ag_2\{(S,S)\text{-}^{i}Pr\text{-pybox}\}\{(3aS,3a'S,8aR,8a'R)\text{-indane-pybox}\}]^{2+}$ of one of them is shown in Figure S1. As in the case of complex **4**, no interaction between the silver atoms and triflate anion was observed. On the other hand, as in the cases of complexes **1** and **4**, the two pybox ligands were twisted around the Ag1−Ag2 axis,

DOI: 10.1021/acs.inorgchem.6b01323
Inorg. Chem. XXXX, XXX, XXX−XXX

Table 1. Selected Bond Distances (Å) and Angles (deg) for Silver(I) Complexes 1, 4–6, and 9–11 and Gold(I) Complex 13

Complex **1**			
Ag1–N1	2.203(6)	Ag2–N3	2.183(6)
Ag1–N2	2.855(6)	Ag2–N5	2.510(6)
Ag1–N4	2.191(6)	Ag2–N6	2.189(6)
Ag1–N5	3.116(6)	Ag1–O5	2.562(10)
Ag2–N2	2.647(6)	Ag1–Ag2	2.8885(9)
N1–Ag1–N4	157.4(2)	N3–Ag2–N6	155.1(2)
N4–Ag1–O5	85.3(3)	N3–Ag2–N5	130.3(2)
N1–Ag1–O5	117.3(3)	N6–Ag2–N5	71.7(2)
Complex **4**			
Ag1–N1	2.090(4)	Ag2–N3	2.152(4)
Ag1–N2	3.061(3)	Ag2–N5	2.794(3)
Ag1–N4	2.087(4)	Ag2–N6	2.146(4)
Ag1–N5	3.050(3)	Ag1–Ag2	3.0295(9)
Ag2–N2	2.683(3)		
N1–Ag1–N4	172.78(19)	N3–Ag2–N6	140.54(18)
Complex **5**			
Ag1–N1	2.148(8)	Ag2–N3	2.131(7)
Ag1–N2	2.867(9)	Ag2–N5	3.013(9)
Ag1–N4	2.166(7)	Ag2–N6	2.137(7)
Ag1–N5	2.831(9)	Ag1–Ag2	3.0530(11)
Ag2–N2	2.968(9)		
N1–Ag1–N4	163.0(3)	N3–Ag2–N6	167.6(3)
Complex **6**·0.5CH_2Cl_2			
Ag1–N1	2.541(7)	Ag1–N4	2.562(7)
Ag1–N2	2.416(5)	Ag1–N5	2.417(6)
Ag1–N3	2.652(6)	Ag1–N6	2.561(7)
N2–Ag1–N5	169.9(2)	N1–Ag1–N6	116.8(3)
N1–Ag1–N2	67.6(2)	N2–Ag1–N4	122.6(2)
N1–Ag1–N5	119.0(2)	N4–Ag1–N5	66.7(2)
N2–Ag1–N6	103.5(2)	N1–Ag1–N4	88.4(2)
N5–Ag1–N6	66.9(2)	N4–Ag1–N6	133.5(2)
Complex **9**·CH_2Cl_2			
Ag1–N1	2.479(6)	Ag1–N4	2.479(6)
Ag1–N2	2.508(6)	Ag1–N5	2.496(6)
Ag1–N3	2.836(5)	Ag1–N6	2.581(7)
Complex **9**·CH_2Cl_2			
N2–Ag1–N5	177.31(19)	N2–Ag1–N4	116.56(19)
N1–Ag1–N4	114.1(2)	N1–Ag1–N6	89.12(18)
N1–Ag1–N5	113.94(18)	N4–Ag1–N6	130.2(2)
N4–Ag1–N5	65.6(2)	N5–Ag1–N6	64.7(2)
N1–Ag1–N2	67.01(18)	N2–Ag1–N6	113.00(18)
Complex **10**·CH_2Cl_2			
Ag1–N1	2.270(11)	Ag2–N6	2.316(10)
Ag1–N4	2.263(9)	Ag2–N9	2.252(10)
Ag1–N7	2.285(11)	Ag1–Ag2	3.1020(11)
Ag2–N3	2.266(11)		
N1–Ag1–N4	113.6(4)	N3–Ag2–N6	127.6(4)
N1–Ag1–N7	121.5(4)	N3–Ag2–N9	117.2(4)
N4–Ag1–N7	121.1(4)	N6–Ag2–N9	109.8(4)
Complex **11**·CH_2Cl_2			
Ag1–N1	2.258(13)	Ag2–N6	2.334(15)
Ag1–N4	2.306(15)	Ag2–N9	2.237(15)
Ag1–N7	2.272(14)	Ag1–Ag2	3.1008(18)
Ag2–N3	2.287(15)		
N1–Ag1–N4	114.9(5)	N3–Ag2–N6	123.9(5)
N1–Ag1–N7	125.1(5)	N3–Ag2–N9	121.8(6)
N4–Ag1–N7	116.8(5)	N6–Ag2–N9	110.1(5)
Complex **13**·Et_2O·$2Me_2CO$			
Au1–N1	2.031(12)	Au3–Cl2	2.247(3)
Au1–Cl1	2.254(4)	Au3–N6	2.039(12)
Au2–N3	2.019(12)	Au4–N7	2.036(13)
Au2–N4	2.025(12)	Au4–Cl3	2.251(4)
Au5–N9	2.024(12)	Au4–Au5	3.302(1)
Au5–N10	2.032(11)	Au5–Au6	3.518(1)
Au6–N12	2.008(14)	Au7–Cl5	2.248(10)
Au6–Cl4	2.267(4)	Au7–Cl6	2.230(14)
Au1–Au2	3.474(1)	Au8–Cl7	2.165(18)
Au2–Au3	3.474(1)	Au8–Cl8	2.240(16)
Au3–Au4	3.139(1)		
N1–Au1–Cl1	174.5(4)	N9–Au5–N10	175.7(5)
N3–Au2–N4	175.7(5)	N12–Au6–Cl4	174.2(4)
N6–Au3–Cl2	175.1(4)	Cl5–Au7–Cl6	178.8(3)
N7–Au4–Cl3	177.1(4)	Cl7–Au8–Cl8	179.6(4)

Scheme 2. Synthesis of the Dinuclear Complex 5

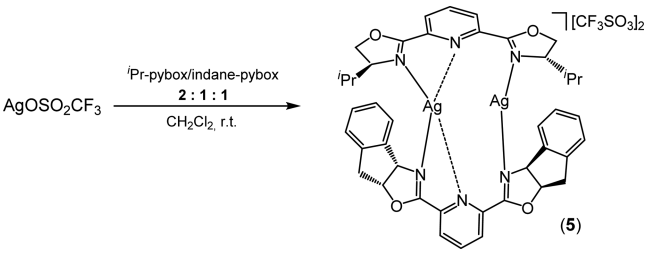

generating a double-heterostranded helicate structure and giving rise to complex **5** as the single diastereoisomer *M* (*S*,*S*)(3a*S*,3a′*S*,8a*R*,8a′*R*).

Synthesis of the Mononuclear Complexes [Ag{(*S*,*S*)-^{i}Pr-pybox}$_2$][X] [X = SbF_6 (6), PF_6 (7), and BF_4 (8)] and [Ag{(3a*S*,3a′*S*,8a*R*,8a′*R*)-indane-pybox}$_2$][BF_4] (9). When the reaction of the silver salts AgX (X = SbF_6, PF_6, and BF_4) and ^{i}Pr-pybox was carried out using a larger amount of the ligand (1:2 molar ratio), in dichloromethane at room temperature, the mononuclear complexes [Ag{(*S*,*S*)-^{i}Pr-pybox)$_2$][X]$_2$ (**6**–**8**, 80–83% yield) were obtained as the sole reaction products. In turn, complex **9** was synthesized by the reaction of AgF, BF_3·OEt_2, and the indane-pybox ligand in dichloromethane at room temperature (1:1:2 molar ratio, 61% yield; Scheme 3).

Following are the selected spectroscopic data: (i) The mass spectra (FAB) of complexes **6** and **9** show the base peak corresponding to the ion molecular [Ag(R-pybox)$_2$]$^+$ at *m*/*z* 709 (**6**) and 893 (**9**). (ii) The molar conductivity values found for complexes **6**–**9** (110–134 S cm^2 mol^{-1}) are in the range as those expected for 1:1 electrolytes.[19] (iii) The presence of a C_2-symmetry axis is evidenced by the room temperature ^{1}H and ^{13}C{^{1}H} NMR studies carried out on complexes **6**–**9**. For instance, complexes **6**–**8** display single ^{13}C{^{1}H} NMR signals for the OCN, OCH_2, and CH^{i}Pr carbon atoms of oxazoline rings and for the C3/C5 and C2/C6 carbon atoms of the pyridine rings of both pybox ligands. The ^{13}C{^{1}H} NMR

DOI: 10.1021/acs.inorgchem.6b01323
Inorg. Chem. XXXX, XXX, XXX–XXX

Scheme 3. Synthesis of the Mononuclear Complexes 6−9

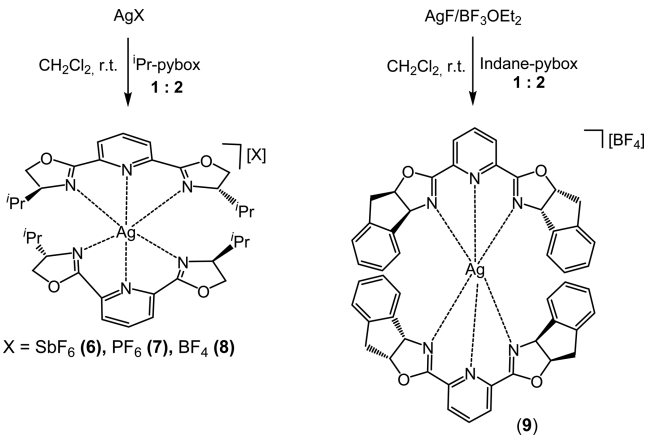

spectrum of complex **9** shows also single resonances for OCN, OCH, and NCH, C3/C5 and C2/C6 carbon atoms of the oxazoline and pyridine rings of both pybox ligands (see the Experimental Section for details). (iv) VT ^{1}H NMR measurements (298−183 K) for complex **6** did not show any splitting of the signals nor did they lead to the observation of other species in solution. The structures of complexes **6** and **9** were confirmed by single-crystal X-ray analysis. An ORTEP-type view of the cation of **6** is shown in Figure 3, and selected

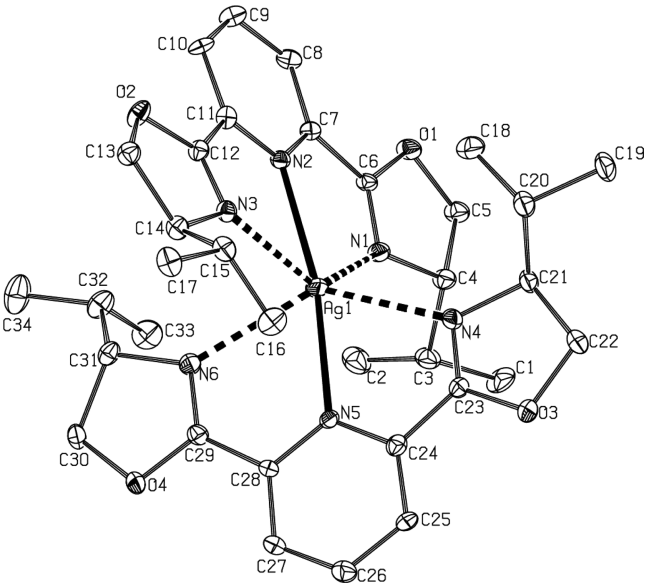

Figure 3. ORTEP drawing of the cationic complex **6** showing the atom-labeling scheme. Thermal ellipsoids are shown at the 20% probability level. Hydrogen atoms and the SbF_6 anion are omitted for clarity.

bonding data of complexes **6** and **9** are shown in Table 1. An ORTEP-type view of the cation of **9** is shown in Figure S2. Both structures show a monomer cation, [Ag{(*S*,*S*)-^{i}Pr-pybox}$_2$]$^+$ or [Ag{(3a*S*,3a′*S*,8a*R*,8a′*R*)-indane-pybox}$_2$]$^+$, and an uncoordinated anion, SbF_6^- (**6**) or BF_4^- (**9**). In both structures, the silver atom is surrounded by a strongly distorted octahedral coordination environment that results from the tridentate coordination of two pybox ligands through the pyridine and oxazoline nitrogen atoms, giving rise to a formal 22-electron complex. However, all Ag−$N_{pyridine}$ and Ag−$N_{oxazoline}$ distances are larger than the sum of the covalent radii of silver and nitrogen atoms (2.16 Å),[23] indicating a weak interaction of both pybox ligands with the silver atom. The oxazoline nitrogen N3 atom lies further away [Ag1−N3 2.652(6) Å for **6** and 2.836(5) Å for **9**], whereas the rest of the Ag−N distances are in the ranges of 2.416(5)−2.562(7) Å for **6** and 2.479(6)−2.581(7) Å for **9**. Both pybox skeletons are near the planarity for **6** and get away somewhat from the planarity for **9**, with the N−C−C−N torsion angles being in the ranges of −3.4(13) to +10.8(13)° (for **6**) and −26.6(9) to −7.2(9)° (for **9**).

On the other hand, the reaction of ^{i}Pr-pybox and the silver salt of a more coordinating anion, $AgOSO_2CF_3$ (2:1 molar ratio), takes place to give a solid that could not be characterized by NMR analysis. Moreover, suitable crystals for X-ray analysis could not be obtained because all attempts of crystallizing this solid resulted in formation of the dinuclear complex **1**.

Synthesis of the Dinuclear Complexes [Ag$_2${(3a*S*,3a′*S*,8a*R*,8a′*R*)-indane-pybox}$_3$][X]$_2$ [X = CF_3SO_3 (10), SbF_6 (11), and PF_6 (12)]. The reaction of the corresponding silver salt AgX (X = CF_3SO_3, SbF_6, and PF_6) and indane-pybox (2:3 molar ratio) in dichloromethane at room temperature led to the dinuclear complexes [Ag$_2${(3a*S*,3a′*S*,8a*R*,8a′*R*)-indane-pybox}$_3$][X]$_2$ (**10**−**12**) in 42−63% yield (Scheme 4).

Scheme 4. Synthesis of the Dinuclear Complexes 10−12

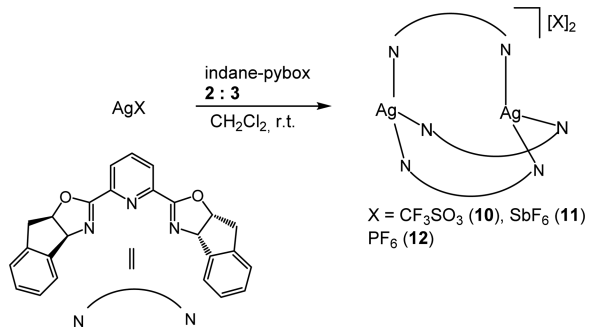

The ^{1}H NMR spectra of complexes **10**−**12** (acetone-d_6, room temperature) show broad peaks, suggesting the presence of a dynamic process in solution (see the NMR Elucidation and Diffusion Studies section for these complexes). The structures of complexes **10** and **11** were confirmed by single-crystal X-ray analysis and consist of a dimeric cation [Ag$_2${(3a*S*,3a′*S*,8a*R*,8a′*R*)-indane-pybox}$_3$]$^{2+}$ and two uncoordinated anions.[30] Both structures are very similar, and therefore only the data corresponding to **10** will be discussed. Selected bonding data of complexes **10** and **11** and an ORTEP-type view of the cation of **10** are shown in Table 1 and Figure 4. An ORTEP-type view of the cation of **11** is shown in Figure S3.

Both silver atoms of **10** have similar coordination environments, being coordinated to three oxazoline nitrogen atoms of different pybox ligands showing a distorted trigonal-planar array [bond angles N_{ox}−Ag1−N_{ox} and N_{ox}−Ag2−N_{ox} in the range of 109.8(4)−127.6(4)°]. Each silver atom is almost located in the plane defined by the three oxazoline nitrogen atoms [+0.256(1) and −0.305(1) Å deviations for Ag1 and Ag2, respectively]. The Ag−$N_{oxazoline}$ bond lengths in complex **10** [range of 2.252(10)−2.316(10) Å] are longer than those found in complex **4**. Among the pyridine nitrogen atoms, it should be noted that the N5 atom is closer to silver atoms [Ag1−N(5)

DOI: 10.1021/acs.inorgchem.6b01323
Inorg. Chem. XXXX, XXX, XXX−XXX

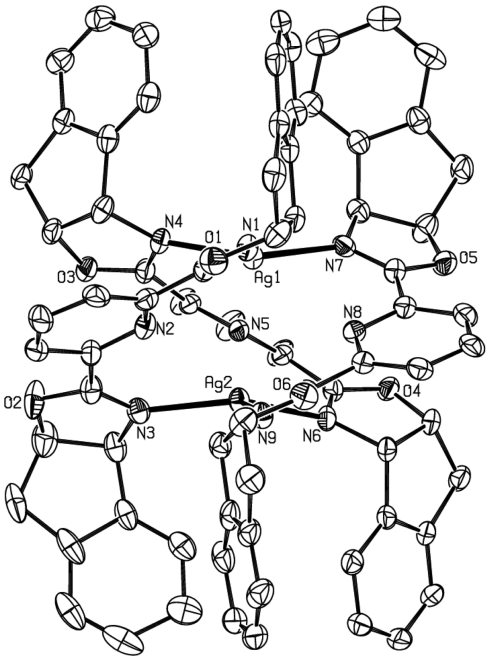

Figure 4. ORTEP drawing of the cationic complex **10** showing the atom-labeling scheme. Thermal ellipsoids are shown at the 20% probability level. Hydrogen atoms and the CF_3SO_3 anions are omitted for clarity.

2.877(9) Å; Ag2−N5 2.753(9)] than the N2 and N8 atoms (av. 3.046(12) Å; range of 2.922(12)−3.127(12) Å), with the Ag−$N_{pyridine}$ distances in all cases being shorter than the sum of the van der Waals radii (3.27 Å).[26]

The Ag1···Ag2 distance [3.1020(11) Å], consistent with an argentophilic interaction between the silver atoms, is slightly larger for complex **10** that for complex **4** [3.029(6) Å]. As in the case of complexes **1** and **4**, the pybox skeleton is not planar, and the pybox ligands are twisted around the Ag1−Ag2 axis, generating a triple-stranded helicate structure.[28b] The N−C−C−N torsion angle values of the pybox ligands are in the range of 20(2)−34(2)°.

Synthesis of the Hexanuclear Gold Complex $[Au_6Cl_4\{(S,S)\text{-}^iPr\text{-pybox}\}_4][AuCl_2]_2$ (13). The reaction of equimolar amounts of complexes $[AuCl\{S(CH_3)_2\}]$ and (*S*,*S*)-^{i}Pr-pybox in acetonitrile at room temperature led diasteroselectively to the hexanuclear complex **13**, which was isolated in moderate yield (43%; Figure 5). The room temperature ^{1}H and $^{13}C\{^1H\}$ NMR spectra of complex **13** are fully consistent with the presence of a C_2-symmetry axis. Thus, the $^{13}C\{^1H\}$ NMR spectrum shows single resonance signals for the OCH_2, OCN, and CH^{i}Pr carbon atoms of both oxazoline rings and for the C3/C5 and C2/C6 carbon atoms of the pyridine ring. The mass spectrum (FAB) of **13** shows the base peak at *m*/*z* 730 ($[Au_2Cl(^iPr\text{-pybox})]^+$). The NMR (^{1}H, ^{13}C, and HSQC experiments) and mass spectrum (FAB) data do not allow one to unambiguously determine the structure of complex **13**. Therefore, single-crystal X-ray analysis was carried out, showing that **13** consists of a hexanuclear dication $[Au_6Cl_4\{(S,S)\text{-}^iPr\text{-pybox}\}_4]^{2+}$ and two mononuclear $[AuCl_2]^-$ anions. The ORTEP-type view of the cation of complex **13** is depicted in Figure 5, and selected bonding data are collected in Table 1. The cation unit is comprised by six gold atoms, four ^{i}Pr-pybox ligands, and four chlorine atoms. The ^{i}Pr-pybox/gold coordination occurs only through the oxazoline nitrogen atoms, and gold atoms do not present the same coordination environment: Au1, Au3, Au4, and Au6 are coordinated to one of the oxazoline nitrogen atoms of the four pybox ligands [Au1−N1, Au3−N6, Au4−N7, and Au6−N12] and to a chlorine atom, whereas Au2 and Au5 are coordinated to the other oxazoline nitrogen atom of the pybox bonded to Au1 and Au3 and to A4 and Au6, respectively. The bonds distances Au−$N_{oxazoline}$ [2.008(14)−2.039(12) Å] and Au−Cl [2.247(3)−

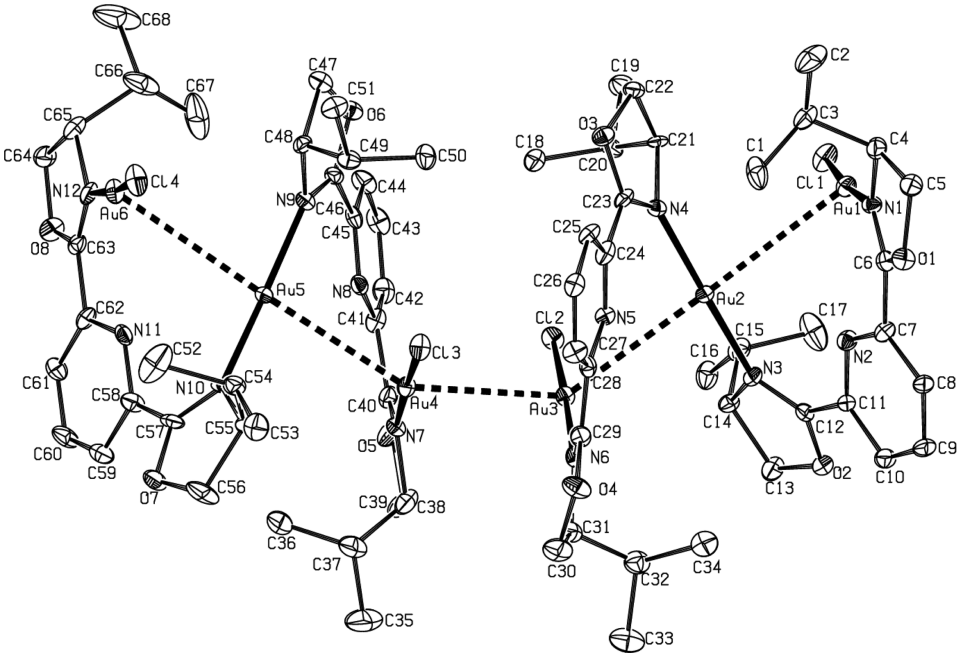

Figure 5. ORTEP drawing of the cationic complex **13** showing the atom-labeling scheme. Thermal ellipsoids are shown at the 20% probability level. Hydrogen atoms and the $[AuCl_2]^-$ anions are omitted for clarity.

DOI: 10.1021/acs.inorgchem.6b01323
Inorg. Chem. XXXX, XXX, XXX−XXX

2.267(4) Å] are within the range found for other gold(I) complexes with oxazoline[31] or chlorine ligands.[32,33]

The gold atoms of complex **13** feature aurophilic interactions and adopt a linear coordination mode with small deviations from the 180° axis [N−Au−Cl or N−Au−N angles between 174.2(4) and 177.1(4)°]. The shortest Au−Au distance [3.139(1) Å] corresponds to Au3···Au4, whereas the other distances are in the range 3.302(1) to 3.518(1) Å. The last one is at the upper end of the generally accepted range of aurophilic interactions.[33,34] On the other hand, the pybox skeletons are not planar, and the four pybox ligands show N−C−C−N torsion angle values between −28(3) and −12(2)°.

All attempts to synthesize other gold/pybox complexes using the same precursor [AuCl{S(CH_3)$_2$}] and other pybox ligands [(*R*,*R*)-Ph-pybox and (*S*,*S*)-^{i}Pr-Pybox-diPh] under different reaction conditions were unsuccessful.

Compound **13** represents, to the best of our knowledge, the sole gold/pybox complex as yet reported.[18]

NMR Elucidation and Diffusion Studies for Complexes 1, 4, 10, and 12. The solid-state characterization of the new silver(I)/pybox complexes **1**, **4**, **10**, and **12** was complemented with a solution-state study by NMR spectroscopy because the catalytic activity of these complexes is always studied in solution. We performed several experiments including structure elucidation, VT measurements, and diffusion studies using diffusion-ordered spectroscopy.

The NMR study of complexes **1** and **4** showed that their crystalline structures (see Figures 1 and 2) are not maintained in solution. Thus, ^{1}H NMR spectra of both complexes **1** and **4** in CD_2Cl_2 at 298 K showed one set of signals for the oxazoline (**1**), indenoxazole (**4**), and pyridine rings of both ligands. This observation is consistent with a fast pyridine ligand exchange between the two silver nuclei that would result in the observed time-averaged C_2-symmetry structure.[35] The unique signal at the ^{19}F NMR spectrum (δ = −78.9 ppm for **1** and −78.8 ppm for **4**) also suggests the same chemical environment for the two triflate anions. Low-temperature measurements in CD_2Cl_2 revealed that the ^{19}F NMR signal does not exhibit any splitting in the ranges of 298−183 K (for **1**) and 298−213 K (for **4**), whereas the splitting of the ^{1}H NMR signals start at 223 K, leading to two sets of peaks at 183 K (80:20 ratio for **1**) and 213 K (85:15 ratio for **4**), which would be in accordance with the presence of two conformer structures in solution.

The possible existence of a dynamic fast coordination process of the two triflate anions was studied through DOSY experiments for complexes **1** and **4**.[36−39] The diffusion coefficients of the cationic complexes and triflate anion were obtained from the ^{1}H and ^{19}F DOSY NMR spectra, respectively. The measured diffusion coefficients of both complexes **1** and **4** at 298 K, the hydrodynamic radii afforded via the Stokes−Einstein equation, and the radii calculated from the X-ray structure are presented in Table 2.

Significantly, the large value of the hydrodynamic radius of the triflate anion in both complexes (**1**, 4.2 Å; **4**, 4.7 Å) versus its X-ray radius (2.75 Å) clearly indicates the existence of an intimate ion pair between the CF_3SO_3 anion with the cation complex. Because the sizes of the cations are much bigger than that of the anion, the values obtained for them are less significant, although they also point in the same direction.

The cation−anion interaction for both complexes **1** and **4** was also corroborated through HOESY NMR experiments.[40] Strong cross peaks between the fluorine atom with the C*H*^{i}Pr (H10) and CH*Me*$_2$ (H13 and H14) proton atoms of the pybox in **1** and with the indane protons (H9, H10, H15, and H16) in **4** in ^{1}H/^{19}F HOESY NMR (see Figure 6) proved that the two ionic fragments behave in a CD_2Cl_2 solution as tight ion pairs. The existence of a unique chemical shift in the ^{19}F NMR spectrum supports the presence of a dynamic process in the dinuclear compounds **1** and **4**, involving a fast triflate anion exchange between the two silver nuclei, causing the two anions to be equivalent and producing a balanced ^{19}F chemical shift and ^{19}F diffusion coefficient values.

Table 2. ^{1}H and ^{19}F DOSY NMR Experiments for Complexes 1 and 4

complex	nucleus	log D (m^2 s^{-1})[a]	r_H (Å)	$r_{X\text{-}ray}$ (Å)
1	^{1}H	−9.07	6.2	6.08[b]/6.27[c]/6.44[d]
1	^{19}F	−8.90	4.2	2.75[e]
4	^{1}H	−9.08	6.3	6.27[f]/6.61[g]
4	^{19}F	−8.95	4.7	2.75[e]

[a]Reported values for a diffusion time parameter Δ = 300 ms. [b][Ag$_2$(^{i}Pr-pybox)$_2$]$^{2+}$. [c][Ag$_2$(CF_3SO_3)(^{i}Pr-pybox)$_2$]$^+$. [d][Ag$_2$(CF_3SO_3)-(^{i}Pr-pybox)$_2$][CF_3SO_3]. [e][CF_3SO_3]. The radius of the triflate anion was calculated from its van der Waals volume. [f][Ag$_2$(indane-pybox)$_2$]$^{2+}$. [g][Ag$_2$(indane-pybox)$_2$][CF_3SO_3]$_2$.

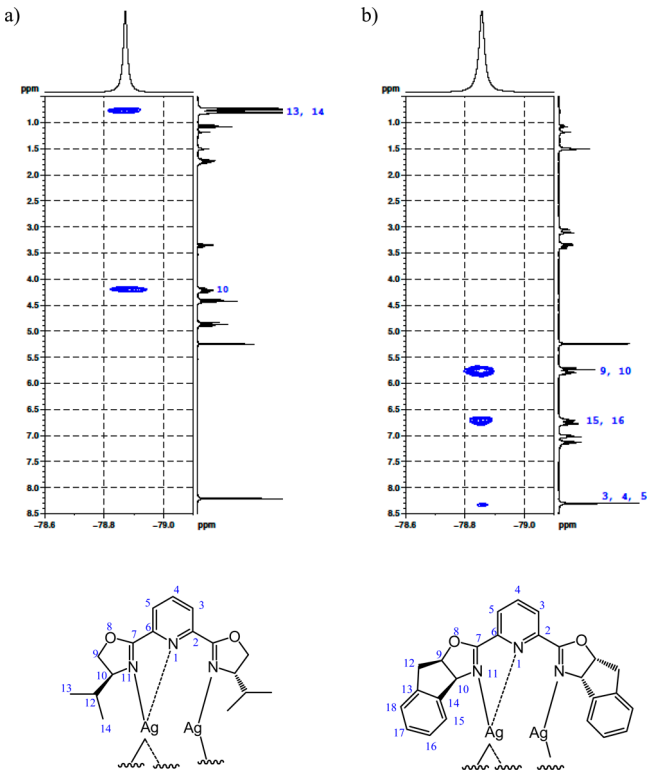

Figure 6. ^{1}H/^{19}F HOESY NMR spectra of complexes (a) **1** and (b) **4**.

A NMR study was also carried out for complexes [Ag$_2$(indane-pybox)$_3$][CF_3SO_3]$_2$ (**10**) and [Ag$_2$(indane-pybox)$_3$][PF_6]$_2$ (**12**). The ^{19}F NMR spectra in CD_2Cl_2 at 298 K showed unique signals at δ = −78.9 ppm (**10**) and −73.2 ppm (**12**), whereas the signal for the PF_6 anion was observed at δ = −144.7 ppm in the ^{31}P NMR spectrum of **12**. However, the ^{1}H NMR spectra at 298 K show a number of broad peaks that suggest the presence of several species in solution (see Figure S4a for **10** and Figure S5a for **12**). When ^{1}H DOSY NMR experiments were accomplished for compounds **10** and **12** at

DOI: 10.1021/acs.inorgchem.6b01323
Inorg. Chem. XXXX, XXX, XXX−XXX

298 K, the same diffusion coefficient was measured for all of the proton signals in each compound (log D = −9.10 and −9.08 m^2 s^{-1} for **10** and **12**, respectively), supporting also the existence of these equilibria at room temperature. As observed for complexes **1** and **4**, heteronuclear NOE contacts between the protons of the cationic fragments and the fluorine atoms of the anions were detected for both the triflate complex **10** and the PF_6 complex **12** through $^1H/^{19}F$ HOESY experiments (see the Supporting Information), which again indicates the existence of tight ion pairs. When the temperature was decreased from 298 to 193 K (Figure S4), the ^1H NMR broad peaks of complex **10** sharpened and two species were observed in an approximate 90:10 ratio, while no splitting for the ^{19}F NMR signal was observed in the same range of temperatures. The major compound was identified, after analysis of the COSY, TOCSY, HSQC, HMBC, and ^{13}C NMR spectra at 213 K, as the three-ligand cationic complex $[Ag_2(indane\text{-}pybox)_3]^{2+}$ **10**.[41] The ^1H NMR spectrum at 213 K of complex **10** shows one set of signals for the six oxazoline and three pyridine rings of the three pybox moieties, denoting a high degree of symmetry in the cationic complex. The minor species was identified as the major conformer of the two-ligand complex $[Ag_2(indane\text{-}pybox)_2][CF_3SO_3]_2$ (**4**). The ratio between complexes **10** and **4** varies with the temperature and was measured at 213 K (82:18) and 193 K (90:10).

Also the temperature dependence of complex **12** was studied through several ^1H NMR experiments recorded in CD_2Cl_2 (Figure S5). The broad signals observed at room temperature were resolved at 213 K (Figure S5d) in three sets of peaks. A careful comparison between this spectrum and the spectra of **4** (Figure S5e) and **10** (Figure S4c) at the same temperature revealed that two of the three sets of peaks observed for **12** also appeared in the ^1H NMR spectrum of complex **4**, and therefore they were tentatively assigned to two conformers of the cationic PF_6 complex $[Ag_2(indane\text{-}pybox)_2]^{2+}$ (**L2** and **L2′**). The third set of peaks, which remains unchanged through over the entire range of temperatures evaluated, resembles the ^1H NMR signals of the CF_3SO_3 cationic three-ligand cationic complex **10**, and analysis of the COSY, TOCSY, HSQC, and HMBC NMR spectra confirmed its assignment as the PF_6 cationic three-ligand complex $[Ag_2(indane\text{-}pybox)_3]^{2+}$ **12**. The two conformers (**L2** and **L2′**) are present in nearly equal proportion (51:49) at 213 K. Thus, at 213 K the solution contains a mixture of the three- and two-ligand complexes in a ratio of **12**:**L2**:**L2′** = 25:38:37.

To confirm the presence of these different size species in solution, DOSY NMR experiments were carried out on the CD_2Cl_2 sample of compound **12**. The ^1H DOSY NMR spectrum of complex **12** measured at 213 K (Figure S6) showed, as expected, two well-defined traces corresponding to two diffusion coefficients, one of which can be assigned to the two-ligand complexes **L2** and **L2′** with a larger diffusion coefficient (D_{L2} = 2.98 × 10^{-10} m^2 s^{-1}) and the other to the three-ligand complex **12** (D_{12} = 2.74 × 10^{-10} m^2 s^{-1}). The calculated ratio from the measured diffusion coefficients (D_{L2}/D_{12} = 1.1) agrees with the expected ratio for the two molecules having two- and three-coordinated indane-pybox ligands [$(MW_{12}/MW_{L2})^{1/3}$; see Table 3].

The results of the DOSY NMR experiments at 298 and 213 K suggest that complex **12** maintains a dynamic equilibrium with its corresponding two-ligand complexes **L2** and **L2′** at room temperature, which is resolved at 213 K. In addition, the 2D ROESY NMR spectra of complex **12** recorded at 213 K showed exchange cross peaks between the parent signals of the two-ligand conformers (**L2** and **L2′**), but no exchange peaks were detected between the resonances of the $[Ag_2(indane\text{-}pybox)_3]^{2+}$ **12** and the $[Ag_2(indane\text{-}pybox)_2]^{2+}$ **L2**/**L2′** species. These observations show that at 213 K the two-ligand complex exists in solution as two exchangeable conformers, but the two different sized complexes do not experience any observable interconversion process.

Table 3. ^1H DOSY NMR Experiments for Complex 12

species in solution	D (×10^{-10} m^2 s^{-1})	D_{L2}/D_{12}	$(MW_{12}/MW_{L2})^{1/3}$
L2 and **L2′**	2.98	1.1	1.12[a]/1.09[b]
12	2.74		

[a]Ratio for $[Ag_2(indane\text{-}pybox)_2]^{2+}/[Ag_2(indane\text{-}pybox)_3]^{2+}$. [b]Ratio for $[Ag_2(indane\text{-}pybox)_2][PF_6]_2/[Ag_2(indane\text{-}pybox)_3][PF_6]_2$. Interactions between the PF_6 anions and the cation fragments in **L2**, **L2′**, and **12** may be assumed to occur in solution, as was previously detected from the $^1H^{19}F$ HOESY NMR spectrum of these species at 298 K.

In conclusion, the three-ligand complexes $[Ag_2(indane\text{-}pybox)_3][X]_2$ **10** and **12** exist in CD_2Cl_2 solution together with variable amounts of their corresponding two-ligand complexes $[Ag_2(indane\text{-}pybox)_2][X]_2$. On the other hand, the anions PF_6 and CF_3SO_3 have different abilities to stabilize the two- or three-ligand complexes. At 213 K, the triflate counteranion favors the three-ligand complex, while for PF_6, it is the two-ligand structure that is the one preferred. Also, the anion significantly affects the ratio of the conformers of the two-ligand complexes. Thus, in the case of complex **10** (X = CF_3SO_3), a highly preferred conformation is observed at low temperature. However, for complex **12** (X = PF_6), the two-ligand complex conformers **L2** and **L2′** are present in a nearly equimolar ratio.

Silver(I)-Catalyzed Addition of Alkynes to Imines. Probably, the addition of terminal alkynes to either imines[12a−e,42] or aldehydes/amines[12h,i,43] catalyzed by transition metals can be considered as the most useful direct access to enantiopure propargylamines. The synthetic potential of these species is well recognized because they have been extensively employed for the construction of privileged nitrogen-containing structures, particularly biologically active compounds and natural products. Recently, we reported the efficient alkynylation reaction of imines catalyzed by the dinuclear complexes $[Cu_2\{(R,R)\text{-Ph-pybox}\}_2][X]_2$ (X = CF_3SO_3 and PF_6; up to 89% e.e.).[2,44] In this paper, we report the results on the addition of phenylacetylene to *N*-benzylideneaniline catalyzed by the new silver(I)/pybox complexes **1**, **2**, **4**, and **10**. In a typical experiment, dried and deoxygenated CH_2Cl_2 (0.5 mL) was placed in a three-neck Schlenk flask, under an argon atmosphere, followed by the addition of the precatalyst (0.02 mmol). After the addition of *N*-benzylideneaniline (0.4 mmol) and phenylacetylene (0.6 mmol), the resulting mixture was stirred in the absence of light (48 h, room temperature) to provide *N*-(1,3-diphenyl-2-propynyl)aniline. As summarized in Table 4, the results of this screening reveal that the catalytic activity of these complexes is only moderate.

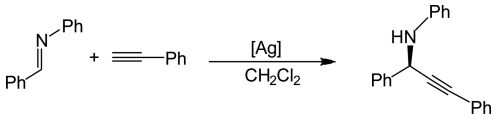

DOI: 10.1021/acs.inorgchem.6b01323
Inorg. Chem. XXXX, XXX, XXX−XXX

Table 4. Catalytic Activity of Dinuclear Silver(I) Complexes for the Enantioselective Synthesis of (1,3-Diphenyl-2-propynyl)aniline[a]

	catalyst	conv (%)	yield (%)[b]	e.e. (%) (*R*)[c]
1	**1**	99	89	24
2	**2**	59	50	26
3	**4**	97	86	44
4	**10**	86	75	40
5	**4**[d]		69	34
6	**4**[e]		76	8
7	**4**[f]		78	14

[a]The reactions were carried out using benzylideneaniline (0.4 mmol). The ratio of benzylideneaniline:phenylacetylene:silver complex = 1:1.5:0.05. The reactions were carried out in anhydrous CH_2Cl_2 (0.5 mL), under an argon atmosphere, in the absence of light, at room temperature for 48 h. [b]Isolated yield after chromatographic purification. [c]Enantiomeric excess determined by HPLC with a Chiralcel OD-H column. The absolute configuration was assigned on the basis of the literature data. [d]Similar reaction conditions in CH_2Cl_2 (0.25 mL) for 24 h. [e]Similar reaction conditions in $CHCl_3$ (0.25 mL) for 24 h. [f]Similar reaction conditions in $CHCl_3$ (0.10 mL) for 6 h.

The resulting *N*-(1,3-diphenyl-2-propynyl)aniline was obtained in high chemical yield when triflate complexes were utilized as catalysts (entries 1 and 3 vs 2). Also, we observed that silver (3a*S*,3a′*S*,8a*R*,8a′*R*)-indane-pybox complexes provide higher enantioselectivity than (*S*,*S*)-^{i}Pr-pybox derivatives (entry 3 vs 1 and 2). The best results were reached using the dinuclear triflate complexes **4** and **10** (entries 3 and 4).

Moreover, it has been reported that both the yield and e.e. of the catalytic addition of phenylacetylene to imines are strongly affected by the solvent.[12c,45] Thus, Kesavan and co-workers observed that the best results for the copper(I)-catalyzed addition of phenylacetylene to benzylidene(*p*-methoxyaniline) were obtained using chlorinated solvents (CH_2Cl_2 and, particularly, $CHCl_3$). In this context, we have checked the solvent effect for catalyst **4** using CH_2Cl_2 and $CHCl_3$ and different concentrations. The use of $CHCl_3$ significantly decreases the e.e. compared with CH_2Cl_2 (entries 6 and 7 vs 3 and 5). In addition, increasing the reagent concentration (CH_2Cl_2, 0.25 mL; $CHCl_3$, 0.25 or 0.1 mL) leads to poorer results in terms of conversion and/or asymmetric induction (entries 5−7 vs 3), although the reaction time is substantially reduced.

Table 5. Crystal Data and Structure Refinement for Complexes 1, 4, and 5

	1	4	5
empirical formula	$C_{36}H_{46}N_6F_6O_{10}S_2Ag_2$	$C_{52}H_{38}N_6F_6O_{10}S_2Ag_2$	$C_{44}H_{42}N_6F_6O_{10}S_2Ag_2$
fw	1116.64	1300.74	1208.69
temperature (K)	173(2)	100(2)	123(2)
wavelength (Å)	1.5418	1.5418	1.5418
cryst syst	orthorhombic	orthorhombic	monoclinic
space group	$P2_12_12_1$	$P2_12_12_1$	$P2_1$
a (Å)	13.5986(1)	12.8183(2)	18.8039(3)
b (Å)	21.2402(2)	16.1215(2)	12.5654(1)
c (Å)	31.0125(3)	23.4147(4)	21.0568(3)
α (deg)	90	90	90
β (deg)	90	90	111.442(2)
γ (deg)	90	90	90
volume (Å^3)	8957.56(14)	4838.65(13)	4630.92(12)
Z	8	4	4
ρ_{calcd} (Mg m^{-3})	1.656	1.786	1.734
μ (mm^{-1})	8.634	8.110	8.412
F(000)	4512	2608	2432
cryst size (mm^3)	0.072 × 0.120 × 0.255	0.121 × 0.095 × 0.046	0.144 × 0.105 × 0.04
θ range (deg)	2.850−74.126	3.931−69.463	3.954−74.626
index ranges	$-16 \le h \le 15$	$-15 \le h \le 5$	$-23 \le h \le 23$
	$-22 \le k \le 25$	$-16 \le k \le 19$	$-15 \le k \le 15$
	$-37 \le l \le 26$	$-28 \le l \le 26$	$-26 \le l \le 25$
no. of reflns collected	28254	20406	37484
no. of indep reflns	14770 [*R*(int) = 0.0399]	8865 [*R*(int) = 0.0378]	18384 [*R*(int) = 0.0490]
completeness (%) (θ)	99.6 (67.000)	99.5 (67.680)	99.9 (67.684)
refinement method	full-matrix least squares on F^2	full-matrix least squares on F^2	full-matrix least squares on F^2
no. of param/restraints	1121/15	703/0	1269/48
GOF on F^2	1.025	1.046	1.017
weight function (*a*, *b*)	0.0728, 6.9205	0.0359, 3.0954	0.0777, 3.8685
R [$I > 2\sigma(I)$][a]	R1 = 0.0442, wR2 = 0.1175	R1 = 0.0348, wR2 = 0.0790	R1 = 0.0520, wR2 = 0.1304
R (all data)	R1 = 0.0472, wR2 = 0.1218	R1 = 0.0404, wR2 = 0.0829	R1 = 0.0635, wR2 = 0.1416
absolute structure param	−0.011(5)	−0.020(4)	−0.030(8)
largest diff peak and hole (e Å^{-3})	1.239 and −1.264	0.635 and −1.174	1.163 and −1.177

[a]$R1 = \sum(|F_o| - |F_c|)/\sum|F_o|$; $wR2 = \{\sum[w(F_o^2 - F_c^2)^2]/\sum[w(F_o^2)^2]\}^{1/2}$.

DOI: 10.1021/acs.inorgchem.6b01323
Inorg. Chem. XXXX, XXX, XXX−XXX

CONCLUSIONS

The synthesis of enantiopure mono- and dinuclear silver(I)/pybox complexes, $[AgL_2]^{2+}$ (L = ^{i}Pr-pybox and indane-pybox), $[Ag_2L_2]^{2+}$ (L = ^{i}Pr-pybox and indane-pybox), and $[Ag_2L_3]^{2+}$ (L = indane-pybox), has been carried out from silver salts and pybox ligands in the appropriate molar ratio. The structures of the dinuclear (**1**, **4**, **5**, **10**, and **11**) and mononuclear (**6** and **9**) silver complexes have been determined by single-crystal X-ray diffraction analysis. From the VT-NMR study of complexes, it can be derived that for complexes **1** and **4** two conformers are present in the solution and that the three-ligand complexes $[Ag_2(\text{indane-pybox})_3][X]_2$ **10** (X = CF_3SO_3) and **12** (X = PF_6) exist in CD_2Cl_2 solution together with variable amounts of their corresponding two-ligand complexes $[Ag_2(\text{indane-pybox})_2][X]_2$. The dinuclear complexes **1**, **2**, **4**, and **10** were tested as catalysts in the addition of phenylacetylene to benzylideneaniline, and complexes **4** and **10** were found to be the most active catalysts, providing high chemical yields but unsatisfactory chiral induction (e.e. 40−44%). Interestingly, the studies herein reported represent, to the best of our knowledge, the first examples of an asymmetric catalytic reaction using silver(I)/pybox complexes. The synthesis of the first gold(I)/pybox complex **13** is also reported.

EXPERIMENTAL SECTION

General Procedures. The reactions were performed under an atmosphere of dry argon using vacuum-line and standard Schlenk techniques. Solvents were dried by standard methods and distilled under argon before use. The (*S*,*S*)-^{i}Pr-pybox[46] and indane-pybox[47] ligands and the complex $[AuCl\{S(CH_3)_2\}]$[48] were prepared by reported methods. IR spectra were recorded on a PerkinElmer 1720-XFT spectrometer. The conductivities were measured at room temperature, in ca. 5×10^{-4} mol L^{-1} acetone solution, with a with a Crison EC-Meter Basic 30+ conductimeter. Carbon, hydrogen, and nitrogen analyses were carried out with PerkinElmer 240-B and LECO CHNS-TruSpec microanalyzers. Mass spectra (FAB) were determined with a VG-AUTOSPEC mass spectrometer, operating in the positive mode; 3-nitrobenzyl alcohol was used as the matrix. Experimental conditions for NMR experiments are available in the Supporting Information. Coupling constants *J* are given in hertz. Abbreviations used: s, singlet; br s, broad singlet; d, doublet; t, triplet; q, quartet; sept, septuplet; m, multiplet. The following atom labels were used for the ^{1}H and $^{13}C\{^1H\}$ NMR spectroscopic data of the pybox ligands:

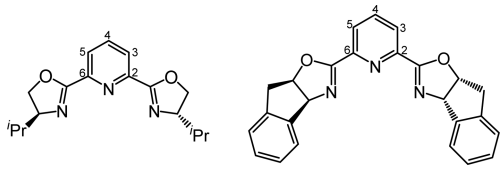

Synthesis of the Dinuclear Complexes $[Ag_2(CF_3SO_3)\{(S,S)\text{-}^i\text{Pr-pybox}\}_2][CF_3SO_3]$ (1), $[Ag_2\{(S,S)\text{-}^i\text{Pr-pybox}\}_2][PF_6]_2$ (2), and $[Ag_2\{(3aS,3a'S,8aR,8a'R)\text{-indane-pybox}\}_2][CF_3SO_3]_2$ (4). The corresponding pybox ligand (0.20 mmol) was added to a suspension of the different silver salts (0.20 mmol) in CH_2Cl_2 (20 mL), and the mixture was stirred, in the absence of light, for 1 h (for **1** and **2**) or 1.5 h (for **4**) at room temperature. Then, the suspension was exposed to light for 1 h, filtered through a cannula transfer, and concentrated under reduced pressure to a volume of ca. 2 mL. The addition of diethyl ether (20 mL; for **1** and **2**) or a mixture of 1:4 diethyl ether/hexane (25 mL; for **4**) afforded a precipitate. The solvents were decanted, and the solid was washed with diethyl ether (3 × 10 mL; for **1** and **2**) or hexane (3 × 10 mL; for **4**) and vacuum-dried.

Complex **1**. Color: colorless. Yield: 84% (0.094 g). Λ_M = 86 S cm^2 mol^{-1} (nitromethane, 293 K). Λ_M = 210 S cm^2 mol^{-1} (acetone, 293 K). IR (KBr): $\nu(CF_3SO_3^-)$ 1265 (vs), 1156 (s), 1026 (vs) cm^{-1}. MS-FAB: *m/z* 709 ($[Ag(^i\text{Pr-pybox})_2]^+$), 408 ($[Ag(^i\text{Pr-pybox})]^+$). $^{19}F\{^1H\}$ NMR (282.40 MHz, CD_2Cl_2, 298 K): δ −78.9. ^{1}H NMR (400.13 MHz, $CDCl_3$, 298 K): δ 8.32 (s, 6H, $H^{3,4,5}$ C_5H_3N), 4.98 (dd, J_{HH} = 9.8 Hz, J_{HH} = 9.1 Hz, 4H, OCH_2), 4.53 (t, J_{HH} = 9.1 Hz, 4H, OCH_2), 4.33 (m, 4H, C*H*^{i}Pr), 1.86 (sept, J_{HH} = 6.7 Hz, 4H,C*H*Me_2), 0.92 (d, J_{HH} = 6.7 Hz, 12H, CH*Me*$_2$), 0.86 (d, J_{HH} = 6.7 Hz, 12H, CH*Me*$_2$). $^{13}C\{^1H\}$ NMR (100.61 MHz, CD_2Cl_2, 298 K): δ 165.5 (s, OCN), 144.2 (s, $C^{2,6}$ C_5H_3N), 140.5 (s, C^4 C_5H_3N), 128.3 (s, $C^{3,5}$ C_5H_3N), 120.4 (q, J_{CF} = 321.0 Hz, $CF_3SO_3^-$), 73.8 (s, OCH_2), 71.7 (s, *C*H^{i}Pr), 32.6 (s, CH*Me*$_2$), 18.7, 18.1 (2s, CH*Me*$_2$). $^{19}F\{^1H\}$ NMR (282.4 MHz, CD_2Cl_2, 298 K): δ −78.3 (s, 3F, $CF_3SO_3^-$). ^{1}H NMR (400.13 MHz, CD_2Cl_2, 193 K): δ 8.29 (br s, 6H, $H^{3,4,5}$ C_5H_3N), 4.92, 4.55, 4.53, 4.21 (4m, 12H, C*H*^{i}Pr, OCH_2), 1.93 (m, 1H, C*H*Me_2), 1.56 (m, 3H, C*H*Me_2), 0.79 (m, 24H, CH*Me*$_2$). $^{13}C\{^1H\}$ NMR (100.61 MHz, CD_2Cl_2, 193 K): δ 165.9, 165.7 (2s, OCN), 143.7, 143.5 (2s, $C^{2,6}$ C_5H_3N), 141.4 (s, C^4 C_5H_3N), 129.1, 128.6 (2s, $C^{3,5}$ C_5H_3N), 120.4 (q, J_{CF} = 321.0 Hz, $CF_3SO_3^-$), 74.9, 72.5, 72.2, 70.2 (4s, *C*H^{i}Pr, OCH_2), 33.7, 31.4 (2s, *C*HMe_2), 19.1, 18.9, 18.2, 16.0 (4s, CH*Me*$_2$). Anal. Calcd for $C_{36}H_{46}N_6F_6O_{10}Ag_2S_2$ (1116.64): C, 38.72; H, 4.15; N, 7.53; S, 5.74. Found: C, 38.78; H, 4.12; N, 7.70; S, 6.04.

Complex **4**. Color: gray. Yield: 67% (0.087 g). Λ_M = 284 S cm^2 mol^{-1} (acetone, 293 K). IR (KBr): $\nu(CF_3SO_3^-)$ 1260 (vs), 1162 (s), 1033 (vs) cm^{-1}. MS-FAB: *m/z* 500 ($[Ag(\text{indane-pybox})]^+$). $^{19}F\{^1H\}$

Table 6. Crystal Data and Structure Refinement for Complexes 6 and 9

	6·0.5CH_2Cl_2	**9**·CH_2Cl_2
empirical formula	$C_{34.5}H_{47}N_6SbClF_6O_4Ag$	$C_{51}H_{40}N_6BCl_2F_4O_4Ag$
fw	988.85	1066.47
temperature (K)	123(2)	100(2)
wavelength (Å)	1.5418	1.5418
cryst syst	monoclinic	monoclinic
space group	C_2	$P2_1$
a (Å)	23.8574(6)	12.818(5)
b (Å)	15.1992(3)	11.676(5)
c (Å)	11.4192(2)	14.992(5)
α (deg)	90	90
β (deg)	103.804(2)	95.998(5)
γ (deg)	90	90
volume (Å^3)	4021.16(15)	2231.5(15)
Z	4	2
ρ_{calcd} (Mg m^{-3})	1.633	1.587
μ (mm^{-1})	10.476	5.340
F(000)	1988	1084
cryst size (mm^3)	0.113 × 0.069 × 0.062	0.177 × 0.163 × 0.151
θ range (deg)	3.478−74.639	2.964−68.302
index ranges	$-29 \le h \le 23$	$-15 \le h \le 15$
	$-18 \le k \le 12$	$-14 \le k \le 14$
	$-11 \le l \le 14$	$-17 \le l \le 17$
no. of reflns collected	7914	30650
no. of indep reflns	5387 [*R*(int) = 0.0299]	7824 [*R*(int) = 0.0272]
completeness (%) (θ)	99.3 (67.000)	99.4 (67.000)
refinement method	full-matrix least squares on F^2	full-matrix least squares on F^2
no. of param/restraints	493/8	622/1
GOF on F^2	1.086	1.057
weight function (*a*, *b*)	0.0537, 0.2962	0.0983, 2.4337
R [$I > 2\sigma(I)$][a]	R1 = 0.0386, wR2 = 0.1042	R1 = 0.0525, wR2 = 0.1411
R (all data)	R1 = 0.0428, wR2 = 0.1087	R1 = 0.0527, wR2 = 0.1414
absolute structure param	0.029(8)	0.006(4)
largest diff peak and hole (e Å^{-3})	0.546 and −1.356	2.067 and −0.688

[a] $R1 = \sum(|F_o| - |F_c|)/\sum|F_o|$. $wR2 = \{\sum[w(F_o^2 - F_c^2)^2]/\sum[w(F_o^2)^2]\}^{1/2}$.

DOI: 10.1021/acs.inorgchem.6b01323
Inorg. Chem. XXXX, XXX, XXX−XXX

Table 7. Crystal Data and Structure Refinement for Complexes 10, 11, and 13

	10·CH_2Cl_2	**11**·CH_2Cl_2	**13**·Et_2O·$2Me_2CO$
empirical formula	$C_{78}H_{59}N_9Cl_2F_6O_{12}S_2Ag_2$	$C_{76}H_{59}N_9Sb_2Cl_2F_{12}O_6Ag_2$	$C_{78}H_{114}N_{12}Cl_8Au_8O_{11}$
fw	1779.10	1952.46	3249.10
temperature (K)	150(2)	150(2)	123(2)
wavelength (Å)	1.5418	1.5418	1.5418
cryst syst	monoclinic	monoclinic	monoclinic
space group	$P2_1$	$P2_1$	$P2_1$
a (Å)	13.6217(5)	13.7551(9)	9.9624(2)
b (Å)	21.2392(8)	21.2733(9)	27.3747(6)
c (Å)	13.9381(6)	13.9694(8)	18.1167(3)
α (deg)	90	90	90
β (deg)	117.097(5)	116.471(8)	95.148(2)
γ (deg)	90	90	90
volume (Å^3)	3589.9(3)	3659.1(4)	4920.81(17)
Z	2	2	2
ρ_{calcd} (Mg m^{-3})	1.646	1.772	2.193
μ (mm^{-1})	6.355	11.484	24.290
F(000)	1800	1928	3032
cryst size (mm^3)	0.216 × 0.087 × 0.048	0.053 × 0.024 × 0.014	0.057 × 0.043 × 0.018
θ range (deg)	3.562−74.414	3.59−74.79	2.93−72.08
index ranges	$-16 \le h \le 12$	$-15 \le h \le 14$	$-12 \le h \le 10$
	$-26 \le k \le 26$	$-25 \le k \le 18$	$-31 \le k \le 32$
	$-16 \le l \le 17$	$-17 \le l \le 16$	$-21 \le l \le 19$
no. of reflns collected	27045	13619	19105
no. of indep reflns	13840 [R(int) = 0.0409]	9391 [R(int) = 0.0432]	14038 [R(int) = 0.0353]
completeness (%) (θ)	100 (67.000)	94.8 (67.00)	96.4 (72.08)
refinement method	full-matrix least squares on F^2	full-matrix least squares on F^2	full-matrix least squares on F^2
no. of param/restraints	989/30	970/22	1066/37
GOF on F^2	1.026	1.088	1.043
weight function (a, b)	0.1279, 2.0533	0.1278, 15.6655	0.0858, 5.8772
R [$I > 2\sigma(I)$][a]	R1 = 0.0685, wR2 = 0.1857	R1 = 0.0774, wR2 = 0.2223	R1 = 0.0476, wR2 = 0.1238
R (all data)	R1 = 0.0864, wR2 = 0.2076	R1 = 0.0851, wR2 = 0.2307	R1 = 0.0506, wR2 = 0.1268
absolute structure param	0.013(6)	0.047(14)	−0.028(15)
largest diff peak and hole (e Å^{-3})	1.169 and −1.227	2.203 and −1.261	2.202 and −2.151

[a] $R1 = \sum(|F_o| - |F_c|)/\sum|F_o|$; $wR2 = \{\sum[w(F_o^2 - F_c^2)^2]/\sum[w(F_o^2)^2]\}^{1/2}$.

NMR (282.40 MHz, CD_2Cl_2, 298 K): δ −78.8. ^{1}H NMR (400.13 MHz, CD_2Cl_2, 298 K): δ 8.42 (s, 6H, H^{3,4,5} C_5H_3N), 7.24 (t, J_{HH} = 7.5 Hz, 4H, CH_{arom}), 7.12 (d, J_{HH} = 7.5 Hz, 4H, CH_{arom}), 6.88 (t, J_{HH} = 7.3 Hz, 4H, CH_{arom}), 6.80 (d, J_{HH} = 7.3 Hz, 4H, CH_{arom}), 5.91 (dd, J_{HH} = 8.7 Hz, J_{HH}= 7.3 Hz, 4H, OCH), 5.83 (d, J_{HH} = 8.7 Hz, 4H, NCH), 3.47 (dd, J_{HH} = 18.4 Hz, J_{HH} = 7.3 Hz, 4H, CH_2), 3.19 (d, J_{HH} = 18.4 Hz, 4H, CH_2). ^{13}C{^{1}H} NMR (100.61 MHz, CD_2Cl_2, 298 K): δ 165.4 (s, OCN), 144.6 (s, C^{2,6} C_5H_3N), 141.0 (s, C^4 C_5H_3N), 139.3, 138.5 (2s, C_{arom}), 129.0 (s, CH_{arom}), 128.3 (s, C^{3,5} C_5H_3N), 127.2, 126.4, 124.1 (3s, CH_{arom}), 120.6 (q, J_{CF} = 319.9 Hz, $CF_3SO_3^-$), 88.1 (s, OCH), 75.6 (s, NCH), 38.8 (s, CH_2). Anal. Calcd for $C_{52}H_{38}N_6F_6O_{10}Ag_2S_2$ (1300.75): C, 48.02; H, 2.94; N, 6.46; S, 4.93. Found: C, 48.13; H, 3.24; N, 6.25; S, 5.13.

*Synthesis of the Dinuclear Complex [Ag$_2${(S,S)-^{i}Pr-pybox}$_2$][BF$_4$]$_2$ (**3**).* Method A: To a suspension of AgF (0.019 g, 0.15 mmol) in dichloromethane (5 mL) were added the ^{i}Pr-pybox ligand (0.045 g, 0.15 mmol) and BF_3·OEt_2 (18 μL, 0.15 mmol). The mixture was stirred at room temperature in the absence of light, for 3 h. Then, the suspension was exposed to light for 1 h, filtered through a cannula transfer, and concentrated under reduced pressure to a volume of ca. 2 mL. The addition of diethyl ether (20 mL) afforded a pale-yellow solid. The solvents were decanted, and the solid was washed with diethyl ether (3 × 5 mL) and vacuum-dried. Method B: The (*S*,*S*)-^{i}Pr-pybox ligand (0.045 g, 0.15 mmol) was added to a suspension of $AgBF_4$ (0.029 g, 0.15 mmol) in dichloromethane (5 mL), and the mixture was stirred at room temperature, in the absence of light, for 3 h. The reaction mixture was worked up as described in Method A. Color: Pale yellow. Yield for method A: 66% (0.049 g). Yield for method B: 70% (0.052 g). Λ_M = 261 S cm^2 mol^{-1} (acetone, 298 K). IR (KBr): ν(BF_4^-) 1064 (vs) cm^{-1}. ^{1}H NMR (400.13 MHz, CD_2Cl_2, 298 K): δ 8.56 (t, J_{HH} = 6.9 Hz, 2H, H^4 C_5H_3N), 8.38 (m, 4H, H^{3,5} C_5H_3N), 5.06 (t, J_{HH} = 9.6 Hz, 4H, OCH_2), 4.68 (t, J_{HH} = 9.6 Hz, 4H, OCH_2), 4.42 (m, 4H, CH^{i}Pr), 1.97 (m, 4H, C*H*Me$_2$), 1.02 (d, J_{HH} = 6.6 Hz, 12H, CH*Me*$_2$), 0.97 (d, J_{HH} = 6.6 Hz, 12H, CH*Me*$_2$). ^{13}C{^{1}H} NMR (100.61 MHz, CD_2Cl_2, 298 K): δ 166.3 (s, OCN), 144.0 (s, C^{2,6} C_5H_3N), 141.7 (s, C^4 C_5H_3N), 126.4 (s, C^{3,5} C_5H_3N), 73.3 (s, OCH_2), 70.9 (s, CH^{i}Pr), 31.4 (s, CHMe$_2$), 17.7, 16.5 (2s, CH*Me*$_2$). ^{19}F{^{1}H} NMR (282.4 MHz, CD_2Cl_2, 298 K): δ −151.3 (s, BF_4^-). Anal. Calcd for $C_{34}H_{46}N_6B_2F_8O_4Ag_2$ (992.12): C, 41.16; H, 4.67; N, 8.47. Found: C, 41.11; H, 4.87; N, 8.13.

*Synthesis of the Dinuclear Complex [Ag$_2${(S,S)-^{i}Pr-pybox}-{(3aS,3a′S,8aR,8a′R)-indane-pybox}][CF$_3$SO$_3$]$_2$ (**5**).* ^{i}Pr-pybox (0.10 mmol) and indane-pybox (0.10 mmol) were added to a suspension of $AgOSO_2CF_3$ (0.052 g, 0.20 mmol) in CH_2Cl_2 (10 mL), and the mixture was stirred, in the absence of light, for 1.5 h at room temperature. Then, the suspension was exposed to light for 1 h, filtered through a cannula transfer, and concentrated under reduced pressure to a volume of ca. 2 mL. The addition of a mixture of 1:4 diethyl ether/hexane (25 mL) afforded a pale-brown precipitate. The solvents were decanted, and the solid was washed with hexane (3 × 10 mL) and vacuum-dried. Color: pale brown. Yield: 56% (0.068 g). Λ_M = 219 S cm^2 mol^{-1} (acetone, 293 K). IR (KBr): ν($CF_3SO_3^-$) 1260 (vs), 1159 (vs), 1029 (s) cm^{-1}. ^{1}H NMR (400.13 MHz, CD_2Cl_2, 298 K): δ 8.44, 8.31 (2m, 6H, H^{3,4,5} C_5H_3N), 7.39 (m, 4H, CH_{arom}), 7.10 (m, 4H, CH_{arom}), 6.07 (d, J_{HH} = 8.4 Hz, 1H, NCH), 6.00 (t, J_{HH} = 7.6 Hz, 1H, OCH), 4.75 (m, 2H, OCH_2), 3.99 (m, 4H, OCH_2, C*H*^{i}Pr),

DOI: 10.1021/acs.inorgchem.6b01323
Inorg. Chem. XXXX, XXX, XXX−XXX

3.72 (dd, J_{HH} = 18.4 Hz, J_{HH} = 7.6 Hz, 2H, CH_2), 3.40 (d, J_{HH} = 18.4 Hz, 2H, CH_2), 0.50 (d, J_{HH} = 6.4 Hz, 6H, CH*Me*$_2$), 0.48 (d, J_{HH} = 6.4 Hz, 6H, CH*Me*$_2$), −0.01 (m, 2H, C*H*Me$_2$). $^{13}C\{^1H\}$ NMR (100.61 MHz, CD_2Cl_2, 298 K): δ 165.3, 165.1 (2s, OCN), 144.7, 144.1 (2s, $C^{2,6}$ C_5H_3N), 140.9, 140.6 (2s, C^4 C_5H_3N), 140.1, 139.4 (2s, C_{arom}), 129.6 (s, CH_{arom}), 128.3 (s, $C^{3,5}$ C_5H_3N), 127.7, 125.7, 125.3 (3s, CH_{arom}), 120.6 (q, J_{CF} = 320.8 Hz, $CF_3SO_3^-$), 87.4 (s, OCH), 75.8 (s, NCH), 73.9 (s, OCH_2), 72.0 (s, CH^{i}Pr), 39.5 (s, CH_2), 32.0 (s, CHMe$_2$), 19.4, 18.2 (2s, CH*Me*$_2$). Anal. Calcd for $C_{44}H_{42}N_6F_6O_{10}Ag_2S_2$ (1208.70): C, 43.72; H, 3.50; N, 6.95; S, 5.30. Found: C, 43.90; H, 3.65; N, 6.81; S, 5.15.

*Synthesis of the Mononuclear Complexes [Ag{(S,S)-^{i}Pr-pybox}$_2$]-[X] [X = SbF$_6$ (**6**), PF$_6$ (**7**), and BF$_4$ (**8**)].* ^{i}Pr-pybox (0.3 mmol) was added to a suspension of the corresponding silver salt (0.15 mmol) in CH_2Cl_2 (20 mL), and the mixture was stirred, in the absence of light, for 1 h at room temperature. Then, the suspension was exposed to light for 1 h, filtered through a cannula transfer, and concentrated under reduced pressure to a volume of ca. 2 mL. The addition of hexane (20 mL) afforded a precipitate. The solvents were decanted, and the solid was washed with hexane (3 × 10 mL) and vacuum-dried.

Complex **6**. Color: pale yellow. Yield: 80% (0.114 g). Λ_M = 134 S cm^2 mol^{-1} (acetone, 293 K). IR (KBr): $\nu(SbF_6^-)$ 656 (vs) cm^{-1}. MS-FAB: *m/z* 709 ([Ag(^{i}Pr-pybox)$_2$]$^+$), 408 ([Ag(^{i}Pr-pybox)]$^+$). $^{19}F\{^1H\}$ NMR (282.40 MHz, CD_2Cl_2, 298 K): δ −124.0. ^1H NMR (600.15 MHz, CD_2Cl_2, 298 K): δ 8.17 (s, 6H, $H^{3,4,5}$ C_5H_3N), 4.63 (dd, 4H, J_{HH} = 9.8 Hz, J_{HH} = 8.7 Hz, OCH_2), 4.53 (t, 4H, J_{HH}= 8.7 Hz, OCH_2), 3.91 (m, 4H, C*H*^{i}Pr), 1.67 (sept, 4H, J_{HH} = 6.7 Hz, C*H*Me$_2$), 0.82 (d, J_{HH} = 6.7 Hz, 12H, CH*Me*$_2$), 0.79 (d, J_{HH} = 6.7 Hz, 12H, CH*Me*$_2$).$^{13}C\{^1H\}$ NMR (100.61 MHz, CD_2Cl_2, 298 K): δ 162.2 (s, OCN), 144.2 (s, $C^{2,6}$ C_5H_3N), 139.7 (s, $C^{3,5}$ C_5H_3N), 125.9 (s, C^4 C_5H_3N), 72.6 (s, OCH_2), 72.1 (s, CH^{i}Pr), 32.6 (s, CHMe$_2$), 18.5, 17.2 (2s, CH*Me*$_2$). Anal. Calcd for $C_{34}H_{46}N_6SbF_6O_4Ag$ (946.40): C, 43.15; H, 4.90; N, 8.88. Found: C, 42.94; H, 4.80; N, 8.90.

*Synthesis of the Mononuclear Complex [Ag{(3aS,3a′S,8aR,8a′R)-indane-pybox}$_2$][BF$_4$] (**9**).* To a suspension of AgF (0.019 g, 0.15 mmol) in dichloromethane (4 mL) were added indane-pybox (0.119 g, 0.30 mmol) and $BF_3{\cdot}OEt_2$ (15 μL, 0.118 mmol). The mixture was stirred at room temperature, in the absence of light, for 3 h. Then, the suspension was exposed to light for 1 h, filtered through a cannula transfer, and concentrated under reduced pressure to a volume of ca. 2 mL. The addition of diethyl ether (25 mL) afforded a solid. Then, the solvents were decanted, and the solid was washed with diethyl ether (3 × 5 mL) and vacuum-dried. Color: pale yellow. Yield: 61% (0.090 g). Λ_M = 110 S cm^2 mol^{-1} (acetone, 293 K). IR (KBr): $\nu(BF_4^-)$ 1059 (mf) cm^{-1}. MS-FAB: *m/z* 893 ([Ag(indane-pybox)$_2$]$^+$), 500 ([Ag-(indane-pybox)]$^+$). ^1H NMR (400.13 MHz, CD_2Cl_2, 298 K): δ 8.32 (d, J_{HH} = 7.6 Hz, 4H, $H^{3,5}$ C_5H_3N), 8.22 (m, 2H, H^4 C_5H_3N), 7.17 (m, 4H, Ph), 7.06−7.00 (m, 12H, Ph), 5.51 (d, J_{HH} = 5.7 Hz, 4H, NCH), 5.12 (m, 4H, OCH), 3.20 (dd, J_{HH} = 18.0, Hz, J_{HH} = 6.0 Hz, 4H, CH_2), 2.88 (d, J_{HH} = 18.0 Hz, 4H, CH_2). $^{13}C\{^1H\}$ NMR (100.61 MHz, CD_2Cl_2, 298 K): δ 162.3 (s, OCN), 144.8 (s, $C^{2,6}$ C_5H_3N), 140.2, 139.5 (2s, C_{arom}), 139.7 (s, C^4 C_5H_3N), 128.8, 127.1 (2s, CH_{arom}), 126.5 (s, $C^{3,5}$ C_5H_3N), 125.4, 125.0 (2s, CH_{arom}), 85.4 (s, OCH), 76.3 (s, NCH), 39.1 (s, CH_2). $^{19}F\{^1H\}$ NMR (282.4 MHz, CD_2Cl_2, 298 K): δ −153.3 (s, BF_4). Anal. Calcd for $C_{50}H_{38}N_6BF_4O_4Ag$ (981.56): C, 61.18; H, 3.90; N, 8.56. Found: C, 60.94; H, 4.15; N, 8.98.

*Synthesis of the Dinuclear Complexes [Ag$_2${(3aS,3a′S,8aR,8a′R)-indane-pybox}$_3$][X]$_2$ [X = CF$_3$SO$_3$ (**10**), SbF$_6$ (**11**), and PF$_6$ (**12**)].* Indane-pybox (0.15 mmol) was added to a suspension of the corresponding silver salt (0.10 mmol) in CH_2Cl_2 (10 mL), and the mixture was stirred, in the absence of light, for 1.5 h at room temperature. Then, the suspension was exposed to light for 1 h, filtered through a cannula transfer, and concentrated under reduced pressure to a volume of ca. 1 mL. The addition of a mixture of 1:4 diethyl ether/hexane (25 mL) afforded a precipitate. Solvents were decanted, and the solid was washed with hexane (3 × 10 mL) and vacuum-dried.

Complex **10**. Color: pale yellow. Yield: 63% (0.053 g). Λ_M = 266 S cm^2 mol^{-1} (acetone, 293 K). IR (KBr): $\nu(CF_3SO_3^-)$ 1262 (vs), 1152 (s), 1030 (vs) cm^{-1}. $^{19}F\{^1H\}$ NMR (282.40 MHz, CD_2Cl_2, 298 K): δ −78.9 (s, 6F, $CF_3SO_3^-$). ^1H NMR (600.15 MHz, Me$_2$CO-*d*$_6$, 298 K): δ 8.51 (m, 9H, $H^{3,4,5}$ C_5H_3N), 7.35 (br s, 12H, CH_{arom}), 6.77 (br s, 6H, CH_{arom}), 6.41 (br s, 6H, CH_{arom}), 5.76 (br s, 6H, OC*H*), 4.39 (br s, 6H, NC*H*), 3.58 (br m, 12H, CH_2). $^{13}C\{^1H\}$ NMR (100.61 MHz, Me$_2$CO-*d*$_6$, 298 K): δ 164.2 (s, OCN), 144.9 (s, $C^{2,6}$ C_5H_3N), 140.9 (s, C^4 C_5H_3N), 140.0, 139.5 (2s, C_{arom}), 129.1 (s, CH_{arom}), 128.8 (s, $C^{3,5}$ C_5H_3N), 125.7, 125.1 (2s, CH_{arom}), 121.0 (q, J_{CF} = 322.0 Hz, $CF_3SO_3^-$), 86.3 (s, OCH), 76.1 (s, NCH), 39.4 (s, CH_2). ^1H NMR (600.15 MHz, CD_2Cl_2, 298 K): δ 8.36 (br s, C_5H_3N), 7.34, 7.21, 7.09, 6.95 (br s, CH_{arom}), 6.68, 6.34 (br s, CH_{arom}), 5.6 (br m, OC*H*), 4.2 (br m, NC*H*), 3.7−2.7 (br m, CH_2). Anal. Calcd for $C_{77}H_{57}N_9F_6O_{12}Ag_2S_2$ (1694.20): C, 54.59; H, 3.39; N, 7.44; S, 3.78. Found: C, 54.28; H, 3.59; N, 7.38; S, 3.98.

Complex **12**. Color: pale yellow. Yield: 63% (0.053 g). Λ_M = 229 S cm^2 mol^{-1} (acetone, 293 K). IR (KBr): $\nu(PF_6^-)$ 843 (vs). $^{19}F\{^1H\}$ NMR (282.40 MHz, CD_2Cl_2, 298 K): δ −73.2 (d, J_{PF} = 712.0 Hz, PF_6^-). ^{31}P NMR (121.5 MHz, CD_2Cl_2, 298 K): δ −144.0 (sp, J_{PF} = 712.0 Hz, PF_6^-). ^1H NMR (400.13 MHz, Me$_2$CO-*d*$_6$, 298 K): δ 8.47 (br s, 9H, $H^{3,4,5}$ C_5H_3N), 7.33 (br s, 12H, CH_{arom}), 6.77 (br s, 6H, CH_{arom}), 6.41 (br s, 6H, CH_{arom}), 5.73 (m, 6H, OCH), 4.39 (br s, 6H, NCH), 3.55 (br s, 12H, CH_2). $^{13}C\{^1H\}$ NMR (100.61 MHz, Me$_2$CO-*d*$_6$, 298 K): δ 164.2 (s, OCN), 144.9 (s, $C^{2,6}$ C_5H_3N), 140.8 (s, C^4 C_5H_3N), 140.0, 139.4 (2s, C_{arom}), 129.1 (s, CH_{arom}), 128.8 (s, $C^{3,5}$ C_5H_3N), 127.9, 125.7, 125.2 (3s, CH_{arom}), 86.3 (s, OCH), 76.2 (s, NCH), 39.4 (s, CH_2). ^1H NMR (600.15 MHz, CD_2Cl_2, 293 K): δ 8.44, 8.34 (br s, $H^{3,4,5}$ C_5H_3N, **12**, **L2**, and **L2′**), 7.35, 7.28, 7.19 (br s, CH_{arom}, **12**, **L2**, and **L2′**), 6.88, 6.75, 6.68 (br s, CH_{arom}, **12**, **L2**, and **L2′**), 6.34 (br s, CH_{arom}, **12**), 5.98, 5.76, 5.58 (br s, OC*H*, **12**, **L2**, and **L2′**, NC*H*, **L2** and **L2′**), 4.12 (br d, *J* = 5.3 Hz, NC*H*, **12**), 3.49, 3.26 (br m, CH_2, **12**, **L2**, and **L2′**). Anal. Calcd for $C_{75}H_{57}N_9F_{12}O_6P_2Ag_2$ (1686.00): C, 53.43; H, 3.41; N, 7.48. Found: C, 53.42; H, 3.66; N, 7.08.

*Synthesis of the Hexanuclear Gold Complex [Au$_6$Cl$_4${(S,S)-^{i}Pr-pybox}$_4$][AuCl$_2$]$_2$ (**13**).* ^{i}Pr-pybox (0.061 g, 0.20 mmol) was added to a solution of [AuCl{S(CH$_3$)$_2$}] (0.059 g, 0.20 mmol) in acetonitrile (20 mL). The solution was stirred, in the absence of light, for 2 h at room temperature and subsequently concentrated under reduced pressure to a volume of ca. 2 mL. The addition of diethyl ether (20 mL) afforded a colorless precipitate. Solvents were decanted, and the solid was washed with diethyl ether (3 × 10 mL) and vacuum-dried. Color: colorless. Yield: 43.5% (0.033 g). Λ_M = 174 S cm^2 mol^{-1} (acetone, 293 K). MS-FAB: *m/z* 730 ([Au$_2$Cl(^{i}Pr-pybox)]$^+$). ^1H NMR (400.13 MHz, CD_2Cl_2, 298 K): δ 8.34 (d, J_{HH} = 7.6 Hz, 8H, $H^{3,5}$ C_5H_3N), 8.17 (m, 4H, H^4 C_5H_3N), 4.83 (m, 8H, OCH_2), 4.65 (m, 16H, OCH_2, C*H*^{i}Pr), 2.68 (m, 8H, C*H*Me$_2$), 1.08 (d, J_{HH} = 7.2 Hz, 24H, CH*Me*$_2$), 1.05 (d, J_{HH} = 6.8 Hz, 24H, CH*Me*$_2$). $^{13}C\{^1H\}$ NMR (100.61 MHz, Me$_2$CO-*d*$_6$, 298 K): δ 165.7 (s, OCN), 143.3 (s, $C^{2,6}$ C_5H_3N), 139.2 (s, C^4 C_5H_3N), 127.9 (s, $C^{3,5}$ C_5H_3N), 72.4 (s, CH^{i}Pr), 71.1 (s, OCH_2), 31.3 (s, CHMe$_2$), 18.2, 14.8 (2s, CH*Me*$_2$). Anal. Calcd for $C_{68}H_{92}N_{12}Cl_8Au_8O_8$ (3064.89): C, 26.65; H, 3.03; N, 5.48. Found: C, 26.51; H, 3.22; N, 5.22.

General Procedure for the Enantioselective Addition of Phenylacetylene to *N*-Benzylideneaniline. Under an argon atmosphere, dried and deoxygenated CH_2Cl_2 (0.5 mL) was placed in a three-neck Schlenk flask, followed by the addition of the dinuclear precatalyst (0.02 mmol). After the addition of *N*-benzylideneaniline (0.4 mmol) and phenylacetylene (0.6 mmol), the resulting mixture was stirred in the absence of light (48 h, room temperature). The volatiles were removed, and the residue was purified by chromatography (silica gel, 5:1 hexane/ethyl acetate). The e.e. of the resulting propargylamine was determined by high-performance liquid chromatography (HPLC; Chiralcel OD-H column, 25 × 0.46 cm) using a 98:2 mixture of hexane/isopropyl alcohol as the eluent [flow rate = 0.5 mL min^{-1}, t_R = 23 min (*R*), and t_R = 27 min (*S*)]. The absolute configuration was assigned on the basis of the literature data.

X-ray Crystal Structure Determination of Complexes 1, 4−6, 9−11, and 13. Suitable crystals for X-ray diffraction analysis were obtained by slow diffusion of a mixture of diethyl ether/hexane into a dichloromethane solution of complexes **1**, **5**, **6**, and **9**−**11**. Mixtures of

DOI: 10.1021/acs.inorgchem.6b01323
Inorg. Chem. XXXX, XXX, XXX−XXX

acetone/hexane (for **4**) or acetone/diethyl ether (for **13**) proved effective for complexes **4** and **13**. The most relevant crystal and refinement data are collected in Tables 5−7.

For **1**, **4**−**6**, **10**, **11**, and **13**, diffraction data were recorded on an Oxford Diffraction Xcalibur Nova (Agilent) single-crystal diffractometer, using Cu Kα radiation (λ = 1.5418 Å). Images were collected at a 65 mm fixed crystal−detector distance, using the oscillation method, with 1° oscillation and variable exposure time per image. The data collection strategy was calculated with the program *CrysAlis Pro CCD*.[49] Data reduction and cell refinement were performed with the program *CrysAlis Pro RED*.[49] An empirical absorption correction was applied using the *SCALE3 ABSPACK* algorithm, as implemented in the program *CrysAlis Pro RED*.[49]

Crystallographic data of **9** were collected using a Bruker Smart 6000 CCD detector and Cu Kα radiation (λ = 1.54178 Å) generated by an Incoatec microfocus source equipped with Incoatec Quazar MX optics. The software *APEX2*[50] was used for the collection of frames of data, indexing of reflections, and determination of lattice parameters, *SAINT*[50] for integration of the intensity of reflections, and *SADABS*[51] for scaling and empirical absorption correction.

The software package *WINGX*[52] was used for space group determination, structure solution, and refinement. The structures of complexes **1**, **5**, **11**, and **13** were solved by Patterson interpretation and phase expansion using *DIRDIF*.[53] The structures of complexes **4**, **6**, **9**, and **10** were solved by direct methods using *SIR92*.[54] In crystals of **6** and **9**−**11**, 0.5 CH_2Cl_2 (for **6**) or 1 CH_2Cl_2 solvent molecule (for **9**−**11**) per unit formula of the complex was present. For **13**, 2 Me_2CO and 1 Et_2O solvent molecules per unit formula of the complex were found. Isotropic least-squares refinement on F^2 using *SHELXL2013*[55] was performed. During the final stages of the refinements, all of the positional parameters and anisotropic temperature factors of all of the non-hydrogen atoms were refined, and the hydrogen atoms were geometrically located and their coordinates refined riding on their parent atoms. The maximun residual electron density was located near heavy atoms.

The function minimized was $[\Sigma w(F_o^2 - F_c^2)/\Sigma w(F_o^2)]^{1/2}$, where $w = 1/[\sigma^2(F_o^2) + (aP)^2 + bP]$ (a and b values are collected in Tables 5−7) from counting statistics and $P = [\max(F_o^2,0) + 2F_c^2]/3$.

Atomic scattering factors were taken from the *International Tables for X-ray Crystallography International*.[56] The crystallographic plots were made with *PLATON*.[57] Geometrical calculations were made with *PARST*.[58]

■ ASSOCIATED CONTENT

Supporting Information

The Supporting Information is available free of charge on the ACS Publications website at DOI: 10.1021/acs.inorgchem.6b01323.

X-ray crystallographic data in CIF format for **1**, **4**−**6**, **9**−**11**, and **13** (CIF)

Experimental conditions for NMR experiments, ORTEP drawing of cationic complexes **5**, **9**, and **11** (Figures S1−S3) and full characterization of complexes **2**, **7**, **8**, and **11**, low-temperature ^{1}H and ^{13}C{^{1}H} NMR spectra for complexes **1**, **4**, **6**, **10**, and **12**, VT-NMR spectra (Figures S4 and S5), ^{1}H DOSY NMR spectrum of complex **12** at 213 K (Figure S6), NMR spectra for compounds **1**, **4**, **6**, **10**, and **12**, including ^{1}H, ^{13}C, ^{31}P, ^{19}F, ^{1}H DOSY, ^{19}F DOSY, COSY, ^{1}H^{13}C HSQC, ^{1}H^{13}C HMBC, ^{1}H^{19}F HOESY, and ROESY at room or variable temperature (PDF)

■ AUTHOR INFORMATION

Corresponding Author

*E-mail: pgb@uniovi.es. Fax: (+34) 985103446.

Notes

The authors declare no competing financial interest.

■ ACKNOWLEDGMENTS

This work was supported by the MICINN of Spain (Grant CTQ2011-26481). E.d.J. thanks the FICYT (Principado de Asturias, Spain) for a predoctoral fellowship (BP12-158).

■ REFERENCES

(1) Desimoni, G.; Faita, G.; Quadrelli, P. *Chem. Rev.* **2003**, *103*, 3119−3154.

(2) Panera, M.; Díez, J.; Merino, I.; Rubio, E.; Gamasa, M. P. *Inorg. Chem.* **2009**, *48*, 11147−11160.

(3) Nakajima, K.; Shibata, M.; Nishibayashi, Y. *J. Am. Chem. Soc.* **2015**, *137*, 2472−2475.

(4) See the Review: Singh, P. K.; Singh, V. K. *Pure Appl. Chem.* **2010**, *82*, 1845−1853.

(5) (a) Gupta, A. D.; Bhuniya, D.; Singh, V. K. *Tetrahedron* **1994**, *50*, 13725−13730. (b) Müller, P.; Boléa, C. *Helv. Chim. Acta* **2001**, *84*, 1093−1111. (c) Müller, P.; Boléa, C. *Synlett* **2000**, 826−828.

(6) Meng, J.-C.; Fokin, V. V.; Finn, M. G. *Tetrahedron Lett.* **2005**, *46*, 4543−4546.

(7) (a) Ginotra, S. K.; Singh, V. K. *Org. Biomol. Chem.* **2006**, *4*, 4370−4374. (b) Ginotra, S. K.; Singh, V. K. *Tetrahedron* **2006**, *62*, 3573−3581 and references cited therein.

(8) Shibata, M.; Nakajima, K.; Nishibayashi, Y. *Chem. Commun.* **2014**, *50*, 7874−7877.

(9) Zhao, L.; Huang, G.; Guo, B.; Xu, L.; Chen, J.; Cao, W.; Zhao, G.; Wu, X. *Org. Lett.* **2014**, *16*, 5584−5587.

(10) Hashimoto, T.; Omote, M.; Maruoka, K. *Angew. Chem., Int. Ed.* **2011**, *50*, 8952−8955.

(11) Dodda, R.; Zhao, C.-G. *Tetrahedron Lett.* **2007**, *48*, 4339−4342.

(12) Addition of alkynes to imines: (a) Zeng, T.; Yang, L.; Hudson, R.; Song, G.; Moores, A. R.; Li, C.-J. *Org. Lett.* **2011**, *13*, 442−445. (b) Fe_3O_4 nanoparticle-supported copper(I)/pybox: Zeng, T.; Yang, L.; Hudson, R.; Song, G.; Moores, A. R.; Li, C.-J. *Org. Lett.* **2011**, *13*, 442−445. (c) Shao, Z.; Wang, J.; Ding, K.; Chan, A. S. C. *Adv. Synth. Catal.* **2007**, *349*, 2375−2379. (d) Ji, J.-X.; Wu, J.; Chan, A. S. C. *Proc. Natl. Acad. Sci. U. S. A.* **2005**, *102*, 11196−11200. (e) Wei, C.; Mague, J. T.; Li, C.-J. *Proc. Natl. Acad. Sci. U. S. A.* **2004**, *101*, 5749−5754. (f) Rosa, J. N. *J. Mol. Catal. A: Chem.* **2004**, *214*, 161−165. (g) Wei, C.; Li, C. J. *J. Am. Chem. Soc.* **2002**, *124*, 5638−5639. One-pot three-component reaction of aldehydes, amines, and alkynes: (h) Bisai, A.; Singh, V. K. *Tetrahedron* **2012**, *68*, 3480−3486. (i) Nakamura, S.; Ohara, M.; Nakamura, Y.; Shibata, N.; Toru, T. *Chem. - Eur. J.* **2010**, *16*, 2360−2362. (j) Shao, Z.; Pu, X.; Li, X.; Fan, B.; Chan, A. S. C. *Tetrahedron: Asymmetry* **2009**, *20*, 225−229. (k) Bisai, A.; Singh, V. K. *Org. Lett.* **2006**, *8*, 2405−2408. (l) Wei, C.; Li, Z.; Li, C.-J. *Synlett* **2004**, 1472−1483.

(13) Li, Z.; Jiang, Z.; Su, W. *Green Chem.* **2015**, *17*, 2330−2334.

(14) Singh, P. K.; Singh, V. K. *Org. Lett.* **2008**, *10*, 4121−4124.

(15) (a) $AgOSO_2CF_3$/(*S*,*S*)-R-pybox (R = ^{i}Pr, Ph, and ^{t}Bu) mixtures have been used for the asymmetric kinetic resolution of phenyl-2,3-allen-1-ol with low efficiency (20% conversion, no e.e.): Wang, Y.; Zheng, K.; Hong, R. *J. Am. Chem. Soc.* **2012**, *134*, 4096−4099. (b) The asymmetric catalytic addition of 4-phenyl-1-butyne to the α-imino ester PMP-N=CH(CO_2Et) (PMP = *p*-methoxyphenyl) was explored using silver salts ($AgOSO_2CF_3$ and $AgNO_3$) and several chiral ligands (including pybox). Unfortunately, no chiral induction, as well as extremely low conversions, was observed in all cases (see ref 12d).

(16) (a) Díez, J.; Gamasa, M. P.; Panera, M. *Inorg. Chem.* **2006**, *45*, 10043−10045. (b) Panera, M.; Díez, J.; Merino, I.; Rubio, E.; Gamasa, M. P. *Eur. J. Inorg. Chem.* **2011**, *2011*, 393−404. (c) Gadissa Gelalcha, F. G.; Schulz, M.; Kluge, R.; Sieler, J. *J. Chem. Soc., Dalton Trans.* **2002**, 2517−2521.

(17) Provent, C.; Hewage, S.; Brand, G.; Bernardinelli, G.; Charbonnière, L. J.; Williams, A. F. *Angew. Chem., Int. Ed. Engl.* **1997**, *36*, 1287−1289.

DOI: 10.1021/acs.inorgchem.6b01323
Inorg. Chem. XXXX, XXX, XXX−XXX

(18) Attempts to prepare a gold(III)/pybox complex by the reaction of (*R*,*R*)-Ph-pybox with $Na[AuCl_4]$ in acetonitrile/H_2O were not successful, but a gold(III) amido complex, resulting from a ring-opening reaction of the oxazoline ring, was formed. Corma, A.; Domínguez, I.; Doménech, A.; Fornés, V.; Gómez García, C. J.; Ródenas, T.; Sabater, M. J. *J. Catal.* **2009**, *265*, 238−244.
(19) Geary, W. J. *Coord. Chem. Rev.* **1971**, *7*, 81−122.
(20) (a) Flack, H. D.; Bernardinelli, G. *J. Appl. Crystallogr.* **2000**, *33*, 1143−1148. (b) Flack, H. D. *Helv. Chim. Acta* **2003**, *86*, 905−921. (c) Flack, H. D.; Bernardinelli, G. *Chirality* **2008**, *20*, 681−690.
(21) A linear coordination of silver ions by two oxazoline nitrogen atoms of two different pybox ligands was reported in the complex $[Ag_2\{(S,S)\text{-Bz-pybox}\}_2][BF_4]_2$ [av. N−Ag−N 177(2)° and av. Ag−$N_{oxazoline}$ 2.18(2) Å; see ref 17].
(22) (a) Vega, E.; de Julián, E.; Borrajo, G.; Díez, J.; Lastra, E.; Gamasa, M. P. *Polyhedron* **2015**, *94*, 59−66. (b) Liu, C.; Zhao, Y.; Zhai, L.-L.; Lv, G.-C.; Sun, W.-Y. *J. Coord. Chem.* **2012**, *65*, 165−175. (c) Zhao, Y.; Luo, L.; Liu, C.; Chen, M.; Sun, W. Y. *Inorg. Chem. Commun.* **2011**, *14*, 1145−1148. (d) Wang, Y.-H.; Lee, H.-T.; Suen, M.-C. *Polyhedron* **2008**, *27*, 1177−1184. (e) Ma, S.; Wu, S. *New J. Chem.* **2001**, *25*, 1337−1341.
(23) Cordero, B.; Gómez, V.; Platero-Prats, A. E.; Revés, M.; Echeverría, J.; Cremades, E.; Barragán, F.; Álvarez, S. *Dalton Trans.* **2008**, 2832−2838.
(24) Venkataraman, D.; Lee, S.; Moore, J. S.; Zhang, P.; Hirsch, K. A.; Gardner, G. B.; Covey, A. C.; Prentice, C. L. *Chem. Mater.* **1996**, *8*, 2030−2040.
(25) (aa) Feazell, R. P.; Carson, C. E.; Klausmeyer, K. K. *Inorg. Chem.* **2006**, *45*, 935−944. (b) Feazell, R. P.; Carson, C. E.; Klausmeyer, K. K. *Eur. J. Inorg. Chem.* **2005**, *2005*, 3287−3297. (c) Nilsson, K.; Oskarsson, Å.; Lund, P.-A.; Shen, Q.; Weidlein, J.; Spiridonov, V. P.; Strand, T. G. *Acta Chem. Scand.* **1982**, *36*, 605−610.
(26) Bondi, A. *J. Phys. Chem.* **1964**, *68*, 441−451.
(27) (a) Barreiro, E.; Casas, J. S.; Couce, M. D.; Laguna, A.; López-de-Luzuriaga, J. M.; Monge, M.; Sánchez, A.; Sordo, J.; Vázquez López, E. M. *Dalton Trans.* **2013**, *42*, 5916−5923. (b) Stephenson, A.; Ward, M. D. *Chem. Commun.* **2012**, *48*, 3605−3607. (c) Ray, L.; Shaikh, M. M.; Ghosh, P. *Inorg. Chem.* **2008**, *47*, 230−240.
(28) (a) Mazet, C.; Gade, L. H. *Chem. - Eur. J.* **2002**, *8*, 4308−4318. (b) Piguet, C.; Bernardinelli, G.; Hopfgartner, G. *Chem. Rev.* **1997**, *97*, 2005−2062. (c) Zarges, W.; Hall, J.; Lehn, J.-M.; Bolm, C. *Helv. Chim. Acta* **1991**, *74*, 1843−1852.
(29) Günther, H. *NMR Spectroscopy, Basic principles, concepts, and applications in chemistry*, 2nd ed.; John Wiley: New York, 1995.
(30) A similar species $[Ag_2(R,R\text{-Ph-pybox})_3]^{2+}$ was detected in the ^1H NMR spectrum at 233 K by monitoring a solution of (*R*,*R*)-Ph-pybox with $AgBF_4$ in CD_3CN. The abundance of this complex was maximal for a Ag^+/Ph-pybox ratio of around 0.7 and decreased with increasing Ag^+/Ph-pybox ratio. Under the latter conditions, two other complexes were formed and identified as $[Ag_2(R,R\text{-Ph-pybox})_2]^{2+}$ and $[Ag_3(R,R\text{-Ph-pybox})_3]^{3+}$. Provent, C.; Rivara-Minten, E.; Hewage, S.; Brunner, G.; Williams, A. F. *Chem. - Eur. J.* **1999**, *5*, 3487−3494.
(31) Desmet, M.; Raubenheimer, H. G.; Kruger, G. J. *Organometallics* **1997**, *16*, 3324−3332.
(32) (a) Yeo, W.-C.; Vittal, J. J.; Koh, L. L.; Tan, G.-K.; Leung, P.-H. *Organometallics* **2004**, *23*, 3474−3482. (b) Eggleston, D. S.; Chodosh, D. F.; Girard, G. R.; Hill, D. T. *Inorg. Chim. Acta* **1985**, *108*, 221−226.
(33) Tiekink, E. R. T.; Kang, J.-G. *Coord. Chem. Rev.* **2009**, *253*, 1627−1648.
(34) The Au−Au distances observed in complexes exhibiting aurophilic interactions typically lie between distances observed for the sum of the covalent radii of two Au atoms (2.88 Å) and the two-fold van der Waals radius of gold (ca. 3.60 Å).
(35) Also, a time-average structure with a C_2-symmetry axis was previously observed for the dinuclear complex $[Cu_2\{(S,S)\text{-}^i\text{Pr-pybox}\}_2][PF_6]_2$ (see ref 2).
(36) (a) Morris, K. F.; Johnson, C. S., Jr. *J. Am. Chem. Soc.* **1992**, *114*, 3139−3141. (b) Johnson, C. S., Jr. *Prog. Nucl. Magn. Reson. Spectrosc.* **1999**, *34*, 203−256. (c) Pregosin, P. S.; Kumar, P. G. A.; Fernández, I. *Chem. Rev.* **2005**, *105*, 2977−2998. (d) Claridge, T. D. W. *High Resolution NMR Techniques in Organic Chemistry*, 2nd ed.; Tetrahedron Organic Chemistry Series; Elsevier: Oxford, U.K., 2009; Chapter 9. (e) Morris, G. A. In *Diffusion Ordered Spectroscopy in Multidimensional Methods for the Solution State*; Morris, G. A., Emsley, J. W., Eds.;John Wiley and Sons: Chichester, U.K., 2010; Chapter 36. (f) Will, S. A.; Stait-Gardner, T.; Virk, A. S.; Masuda, R.; Zubkov, M.; Zheng, G.; Price, W. S. In *Modern NMR Techniques for Synthetic Chemistry*; Fisher, J., Ed.; CRC Press: Boca Raton, FL, 2015; p 125.
(37) Stokes−Einstein equation: $D = K_BT/6\pi\eta r_H$, where D = diffusion coefficient, K_B = Boltzmann constant, η = solvent viscosity, and r_H = hydrodynamic radius.
(38) (a) Brand, T.; Cabrita, E. J.; Berger, S. *Prog. Nucl. Magn. Reson. Spectrosc.* **2005**, *46*, 159−196. (b) Pregosin, P. S. *Prog. Nucl. Magn. Reson. Spectrosc.* **2006**, *49*, 261−288. (c) Macchioni, A.; Ciancaleoni, G.; Zuccaccia, C.; Zuccaccia, D. *Chem. Soc. Rev.* **2008**, *37*, 479−489. (d) Pregosin, P. S. *Magn. Reson. Chem.* **2016**, XX DOI: 10.1002/mrc.4394.
(39) (a) Cabrita, E. J.; Berger, S. *Magn. Reson. Chem.* **2002**, *40*, S122−S127. (b) Thureau, P.; Ancian, B.; Viel, S.; Thévand, A. *Chem. Commun.* **2006**, 200−202. (c) Díez, J.; Gimeno, J.; Merino, I.; Rubio, E.; Súarez, F. J. *Inorg. Chem.* **2011**, *50*, 4868−4881.
(40) (a) Drago, D.; Pregosin, P. S.; Pfaltz, A. *Chem. Commun.* **2002**, 286−287. (b) Macchioni, A.; Magistrato, A.; Orabona, I.; Ruffo, F.; Rothlisberger, U.; Zuccaccia, C. *New J. Chem.* **2003**, *27*, 455−458.
(41) Complex **10** is the main complex observed in the ^1H NMR spectrum in acetone-d_6 at 298 K.
(42) (a) Zani, L.; Bolm, C. *Chem. Commun.* **2006**, 4263−4275. (b) Cozzi, P. G.; Hilgraf, R.; Zimmermann, N. *Eur. J. Org. Chem.* **2004**, *2004*, 4095−4105.
(43) (a) Ohara, M.; Hara, Y.; Ohnuki, T.; Nakamura, S. *Chem. - Eur. J.* **2014**, *20*, 8848−8851. (b) Nakamura, S.; Ohara, M.; Nakamura, Y.; Shibata, N.; Toru, T. *Chem. - Eur. J.* **2010**, *16*, 2360−2362. (c) Gommermann, N.; Knochel, P. *Chem. - Eur. J.* **2006**, *12*, 4380−4392.
(44) The structure of complex $[Cu_2\{(R,R)\text{-Ph-pybox}\}_2][PF_6]_2$ was determined by X-ray diffraction, showing the copper atoms to adopt a linear and distorted tetrahedral arrangement as found in the case of the dinuclear silver complex **4** (see ref 2).
(45) Balaraman, K.; Vasanthan, R.; Kesavan, V. *Tetrahedron Lett.* **2013**, *54*, 3613−3616.
(46) Nishiyama, H.; Kondo, M.; Nakamura, T.; Itoh, K. *Organometallics* **1991**, *10*, 500−508.
(47) (a) Jiang, M.; Dalgarno, S.; Kilner, C. A.; Halcrow, M. A.; Kee, T. P. *Polyhedron* **2001**, *20*, 2151−2162. (b) Davies, I. W.; Gerena, L.; Lu, N.; Larsen, R. D.; Reider, P. J. *J. Org. Chem.* **1996**, *61*, 9629−9630.
(48) Brandys, M.-C.; Jennings, M. C.; Puddephatt, R. J. *J. Chem. Soc., Dalton Trans.* **2000**, 4601−4606.
(49) *CrysAlis^{Pro} CCD* and *CrysAlis^{Pro} RED*; Oxford Diffraction Ltd.: Abingdon, Oxfordshire, U.K., 2008.
(50) *APEX2* and *SAINT*; Bruker AXS Inc.: Madison, WI, 2007.
(51) Sheldrick, G. M. *SADABS*; University of Göttingen: Göttingen, Germany, 1996.
(52) Farrugia, L. J. *J. Appl. Crystallogr.* **2012**, *45*, 849−854.
(53) Beurskens, P. T.; Beurskens, G.; de Gelder, R.; Smits, J. M. M.; García-Granda, S.; Gould, R. O.; Smykalla, C. *The DIRDIF Program System, Technical Report of the Crystallographic Laboratory*; University of Nijmegen: Nijmegen, The Netherlands, 2008 (Farrugia, L. J. Windows GUI).
(54) *SIR92*: Altomare, A.; Cascarano, G.; Giacovazzo, C.; Guagliardi, A. *J. Appl. Crystallogr.* **1993**, *26*, 343−350.
(55) Sheldrick, G. M. *SHELXL2013: Program for the Refinement of Crystal Structures*; University of Göttingen: Göttingen, Germany, 2014.
(56) *Tables for X-Ray Crystallography*; Kynoch Press: Birminghan, U.K., 1974; Vol. *IV* (present distributor: Kluwer Academic Publishers: Dordrecht, The Netherlands).
(57) Spek, A. L. *PLATON: A Multipurpose Crystallographic Tool*; University of Utrecht: Utrecht, The Netherlands, 2008.
(58) *PARST*: Nardelli, M. *Comput. Chem.* **1983**, *7*, 95−98.

DOI: 10.1021/acs.inorgchem.6b01323
Inorg. Chem. XXXX, XXX, XXX−XXX